microwave JOURNAL

contents

VOLUME 25, NUMBER 6
USPS 396-250
JUNE 1982

ON THE COVER: Scientific-Atlanta's new millimeter-to-microwave converters adapt 1 - 4 GHz instrumentation receivers to measurements in the 33 to 107 GHz range. The Cover Story begins on page 112.

Press run for this issue is 46,225 copies. *Euro-Global Edition Only.

EXECUTIVE EDITORIAL OFFICE
610 Washington Street, Dedham, MA 02026
Tel: 617 326-8220 710 348-0481
TELEX: 951-659
MICROSOL DEDM

EUROPEAN EDITORIAL OFFICE
25 Victoria Street London SW1H OEH England
Tel: 01-222-0466 **TELEX:** 885744

Microwave Journal is issued without charge upon written request to qualified persons working in that portion of the electronics industry including governmental and university installation that deal with VHF through light frequencies. Other subscriptions; domestic, $36 per year, two year subscriptions $65; foreign, $48 per year, two year subscriptions $85: back issues (if available) and single copies $5.00.

POSTMASTER: send address corrections to Microwave Journal, 610 Washington Street, Dedham MA 02026.

BPA

Horizon House also publishes Telecommunications and Journal of Electronic Defense

mm-Wave Component Tradeoffs For Tactical Systems

C. R. Seashore and D. R. Singh
Honeywell Inc., Millimeter Wave Technology Center
Bloomington, Mn.

Introduction

Future warfare scenarios include land and sea attacks occuring during weather conditions which will place defensive air support at a maximum disadvantage. In adverse weather (rain, fog, snow, haze and low cloud cover) and in battlefield dust or smoke conditions, tactical air strike effectivness can be severely reduced when the visual meterological range falls below 2000 meters. These requirements for new non-electro-optical air-to-surface guidance solutions can be summarized as adverse weather operation, small size compatible with cluster weapon dispersal concepts, low cost and high mission effectiveness. Continuing research and development of the millimeter wavelength region, 30 to 300 GHz, is being carried out for these new guidance solutions because :

- Propagation losses are relatively low in in selected atmospheric windows.
- Reasonable resolution can be obtained from small diameter

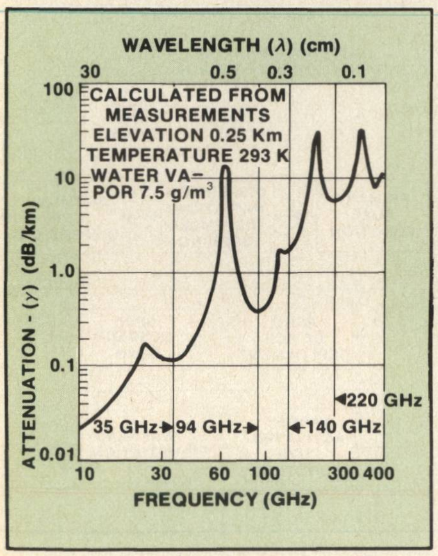

Fig. 1 Characteristics and window frequencies for millimeter wave sensors

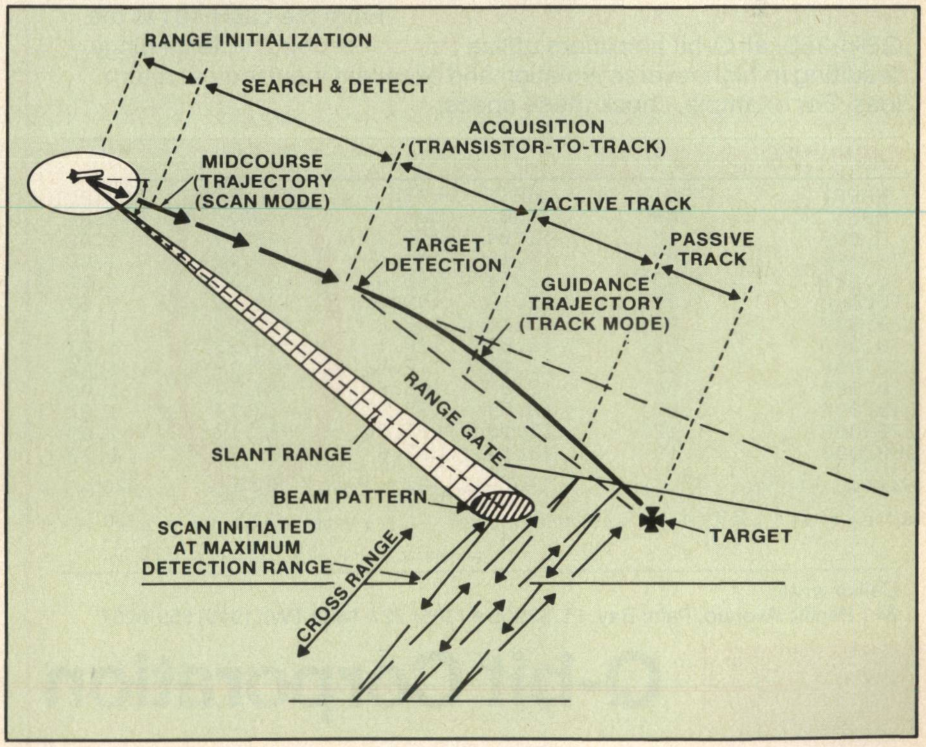

Fig. 2. Millimeter wave active/passive seeker operational sequence.

apertures. For example, a 12 cm diameter antenna provides a 1.8° beamwidth at 94 GHz.

- Tactical targets have significant radar cross sections at millimeter wave frequencies.
- Rapid advances are being made in the development of solid state components and integrated circuit technology up to 110 GHz. However, this could require a major investment in manufacturing techniques to reduce production costs to a tolerable level.

It is in the millimeter wave component area that this paper will put primary emphasis with low cost and producibility being key factors. Indeed, these two factors are driving current component development toward hybrid and monolothic transmit/receive modules for direct interconnection to the antenna feed elements.

Topics to be discussed in this paper include tactical systems, component requirements and relevant integrated circuit techonology.

Tactical Systems

A wide range of system applications utilizing millimeter wave technology are currently being developed. These include precision guided weapons, fire control and target acquisition, ballistic missile defense, communications and remote sensing. They span the frequency spectrum from 30 to 220 GHz. Figure 1 identifies the popular carrier frequencies as well as summarizes some of the important characteristics associated

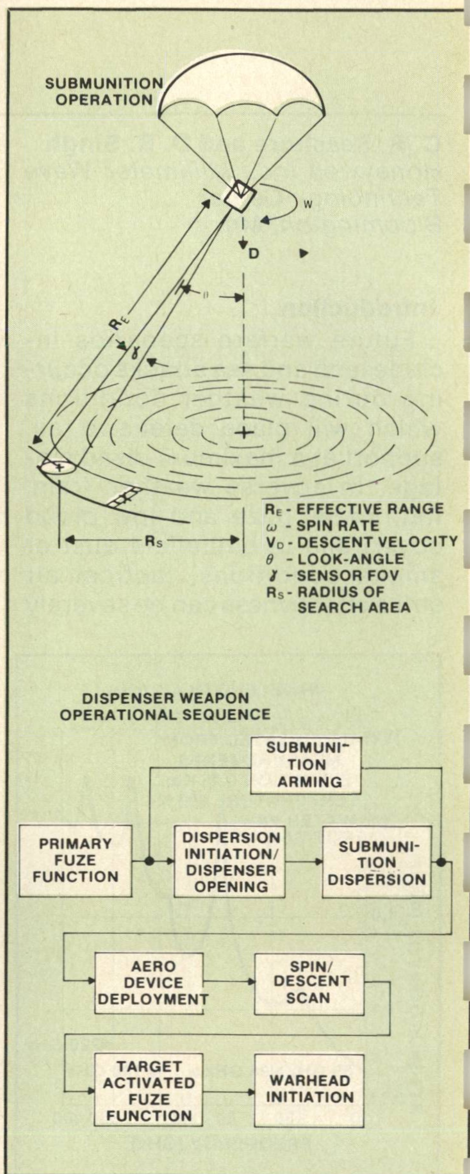

Fig. 3 Sensor fuzed submunition operational sequence.

[Continued on page 44]

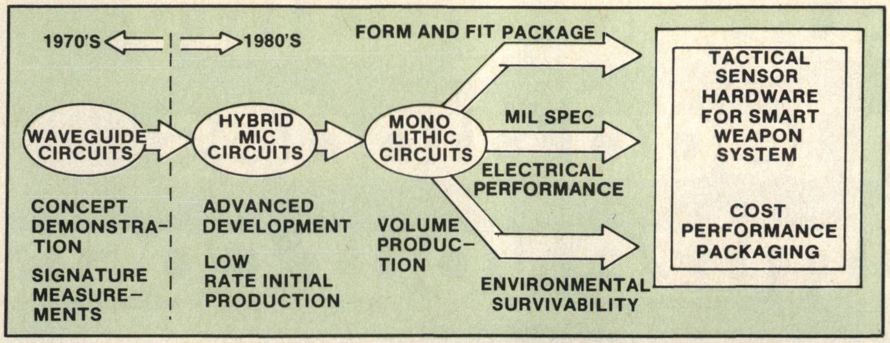

Fig. 4 Millimeter wave component chronology.

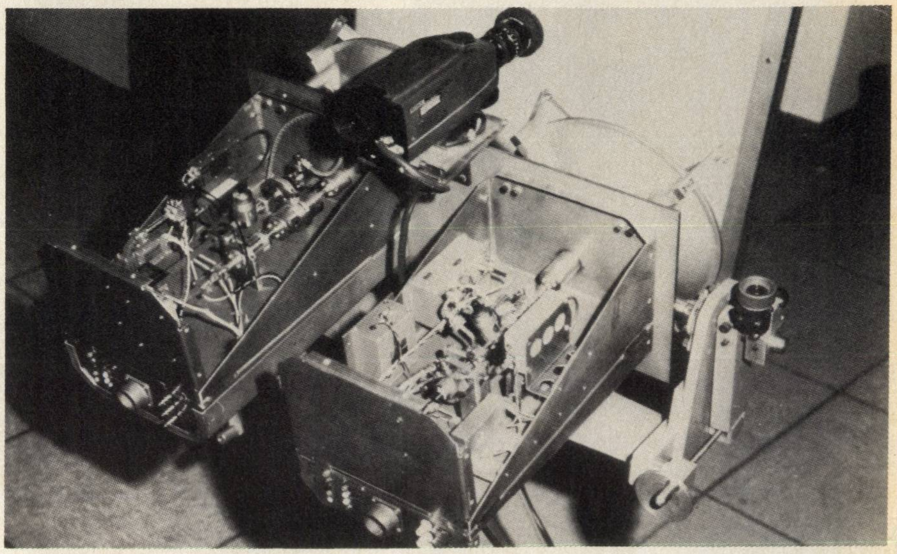

Fig. 5 Dual-frequency 35-95 GHz radars with classical waveguide architecture.

[*Continued on page 46*]

I. MILLIMETER WAVE CIRCUIT TECHNIQUES
RECTANGULAR METAL WAVEGUIDE
HYBRID INTEGRATED CIRCUITS
MICROSTRIP STRIPLINE SUSPENDED STRIPLINE
DIELECTRIC IMAGE GUIDE
MONOLITHIC INTEGRATED CIRCUITS
GALLIUM ARSENDIE SILLICON

II. CONICAL SCAN SEEKER HEAD CHARACTERISTICS FOR Ka-BAND AND W-BAND OPERATION

PARAMETER	K_a -BAND	W-Band
CENTER FREQUENCY	36 GHz	95 GHz
RF BANDWIDTH	2.0 GHz	1.0 GHz
IF BANDWIDTH	900 MHz	800 MHz
TRANSMIT PEAK/POWER	7.5 WATTS	10 WATTS
PULSEWIDTH	60 nsec	50 nsec
PULSE REPETITION FREQUENCY	72 kHz	78 kHz
OPERATION MODES	ACTIVE/PASSIVE	ACTIVE/PASSIVE
ANTENNA DIAMETER	8.0 IN.	5.8 IN.
ANTENNA SIDELOBES	-17 dB	-17 dB
CONSCAN SQUINT	1.5 DEG	0.25 DEG
ANTENNA BEAMWIDTH	3.0 DEG	1.5
CONSCAN RATE	100 Hz	200 Hz
ANTENNA GAIN	34.5 dB	39.5 dB
RANGE GATES	24	48 OVERLAPPED
RANGE GATE WIDTH	60 nsec	50 nsec
SCAN SPEED	60 DEG/SEC	150 DEG/SEC
SCAN LIMITS, AZ	±30 DEG	±20 DEG
SCAN LIMITS, EL	±30 DEG	±10 DEG
	40 DEG	30 DEG

[*Continued on page 48*]

with millimeter wave operation.[1] Of particular interest, due to their volume production potential, are the precision guided weapons (PGW) which can be further subdivided into sensors and seekers. The types of guidance options available for seekers include the following:

a) *Semiactive Guidance* (SAG) - A ground-based or airborne target illuminator radiates the target and the seeker homes in on the target-reflected illuminator signals. Homing may be semiactive all the way or semiactive mid-course followed by active radar and/or passive radiometric terminal guidance.

b) *Lock-On-After Launch* (LOAL) - The seeker autonomously acquires the target and homes on it using active radar and/or passive radiometry.

c) *Lock-On-Before Launch* (LOBL) - The seeker is locked onto the target and launched after the target is initially located by a sensor on the same platform that has launched the seeker-equipped weapon.

d) *Command* (CMD) - The weapon is guided to the target by a sensor which provides either guidance commands or beam rider information to the weapon.

Figure 2 illustrates the operational sequence of a LOAL active/passive seeker whose initial flight profile is essentially parallel to the earth's surface. Target acquisition, detection and tracking are carried out autonomously in the terminal mode by the rapidly descending seeker. Examples of these seeker requirements include the Army Copperhead and Assault Breaker programs, as well as the Air Force WASP program.

The sensor portion of PGW, such as the Army SADARM, is illustrated with the submunition operational sequence Figure 3. Individual cylindrical submunitions or bomblets are fitted with ring vortex parachutes or inflatable ballutes, beneath which they are suspended by an angle of about 45°. As they descend, the parachutes rotate at a set speed, so that the millimeter wave sensor placed in front of the cylinder can scan the ground scene below with a spiral motion. If a target is detected and verified, the sensor immediately provides a firing signal to the warhead. Options for the warhead include both forged fragment and particle stream. Typically, a 15.2 cm antenna at 35 GHz provides a 3 to 4° pencil beam, which is sufficiently narrow to distinguish vehicular targets from background clutter. The antenna is made of a metallized frangible material, so that the lethal mechanism can pass through the antenna with minimum impediment.[2] A key function in this concept is reliable target detection to activate the standoff warhead; no significant guidance is attempted other than that associated with the rotating parachute and its payload.

[Continued on page 50]

Component Requirements

The component requirements for millimeter wave sensors and seekers include high performance, small size, lightweight packaging, survivability in a military environment, minimum power consumption and low unit cost in production quantities. This basically means that it is necessary to eventually produce a moderately sophisticated, expendable RF sensor in the same cost/configuration framework that we now associate with modern electro-optical sensors. Table 1 summarizes the typical circuit techniques available at millimeter frequencies. As shown in Figures 4 and 5, the decade of the 70's was largely spent utilizing waveguide componentry in a variety of millimeter wave programs to achieve concept demonstrations and to obtain signature measurement data. When we entered the decade of the 80's, program emphasis had moved away from the cumbersome waveguide configurations to hybrid MIC's which combined several transmit/receive functions. Looking ahead to the late 80's and early 90's, it seems clear that GaAs monolithic IC's will replace many hybrid designs. It is very important to note from Figure 4 that in the final millimeter wave implementation for a tactical weapon system, low cost is ranked above both performance and packaging.

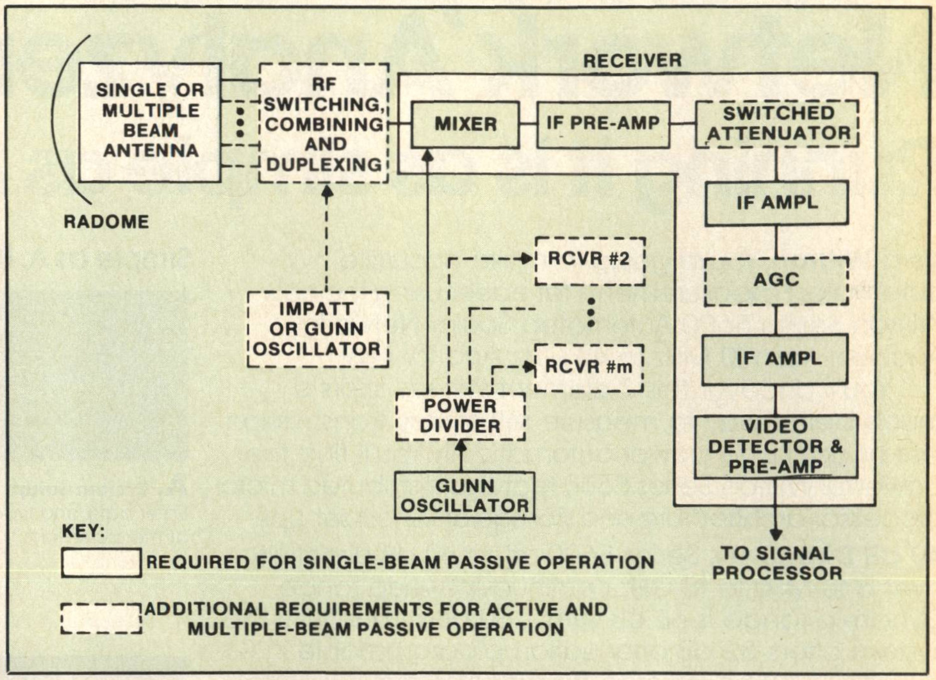

Fig. 6 Generic design for millimeter wave active-passive seeker.

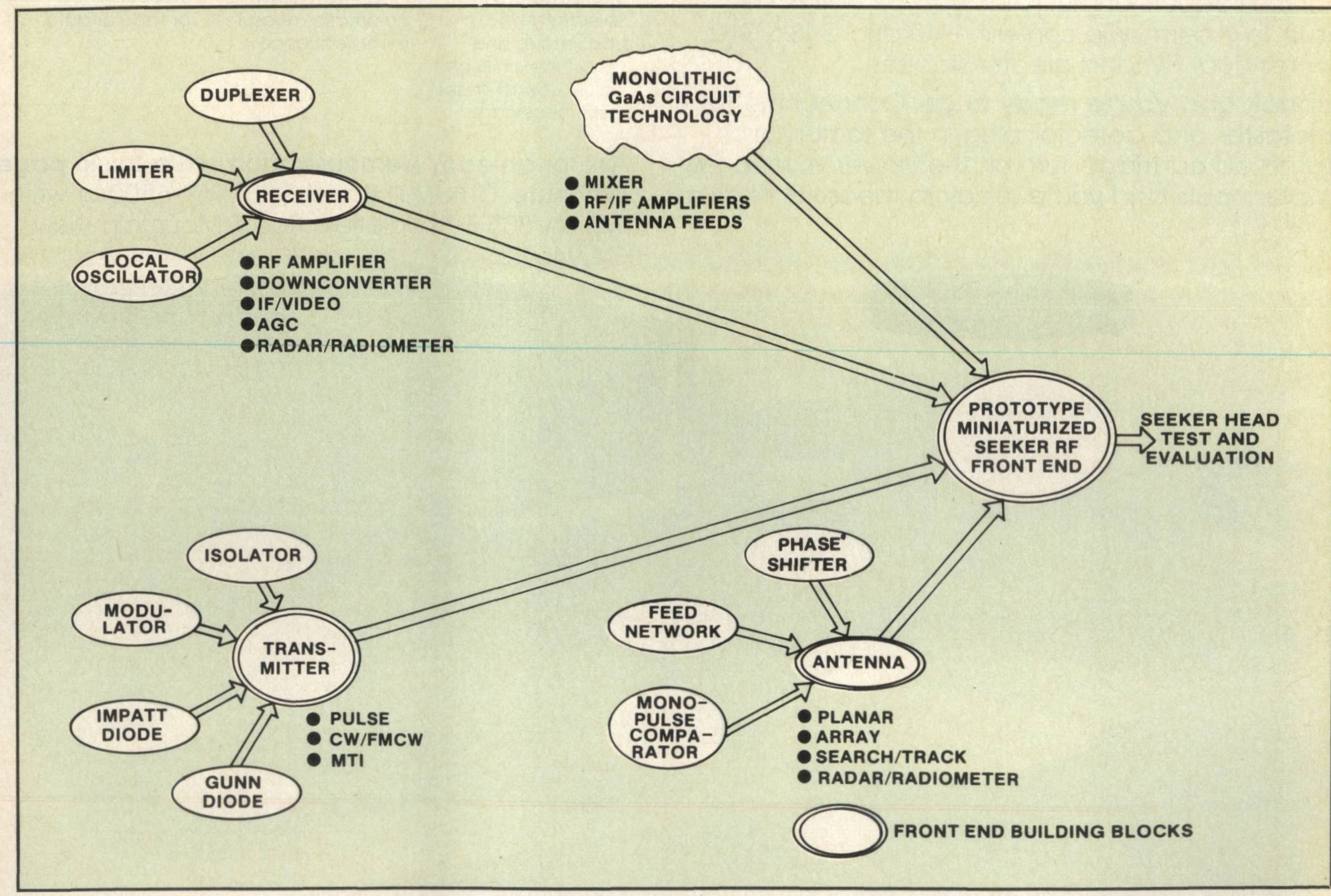

Fig. 7 Anatomy of a miniaturized millimeter wave seeker radar.

[Continued on page 52]

III. Millimeter Wave Hybrid IC Approach

- Integrated Circuit Structures on Low Cost Substrates Such as Duroid 5880
- Microstrip Hybrid Designs Utilizing:
  - Beam Lead Devices
  - Micropill Devices
  - Chip Components
- Modular Packaging for Rapid Test and Evaluation
- CAD Library Developed To:
  - Optimize Electrical Performance
  - Provide Rapid Turn-Around for Design Changes

This reflects current DoD philosophy, particularly in the sensor fuzed submunition application.

A generic functional block diagram for the millimeter wave active/passive seeker is given in Figure 6. This is intended to illustrate the component needs for conical scan and monopulse radar seeker heads as well as for conical scan and multiple channel radiometric seekers. The two predominant solid state sources are IMPATT and a Gunn oscillators, free-running or locked for waveform control. Single downconversion receivers either in single or multiple channel configurations, provide signals for IF and video signal processing. Table II illustrates the key parameters for two conical scan seeker head designs, one operating in Ka-band and the other in W-band. The IMPATT transmitters are operated in a non-coherent, chirp-pulse mode to achieve clutter decorrelation. Miniaturized component requirements apply to the transmitter source and modulator, the duplexer and the single-channel superheterodyne receiver. These component functions are further described in Figure 7. Hybrid circuit integration is currently being actively pursued for each of the three building blocks; receiver, transmitter and antenna. Monolithic GaAs circuit technology is being slowly developed primarily in the mixer, RF/IF amplifier and antenna feed element areas. This monolithic technology is focused in Ka-band at the present time due to device and processing limitations.

Integrated Circuit Technology

The two integrated circuit techniques which are relevent for the millimeter wave tactical sensor/seeker requirements are the hybrid MIC and the monolithic. The hybrid approach best can be described as shown in Table III. It utilizes microstrip transmission lines on a low-cost, soft, substrate and discrete beam lead or micropill semi-conductor devices. Figure 8 illustrates the typical hybrid assembly with microscope and delicate hand-eye coordination. Clearly, this will have to be replaced with computer-aided manufacturing (CAM) techniques if

[Continued on page 54]

the hybrid is to achieve minimal assembly and test labor costs.

Particularly in the hybrid design, a number of device and material tradeoffs need to be made at the various candidate operating frequencies. Table IV illustrates these possibilities for the various transmit/receive components. It should be noted that GaAs and InP device materials become increasingly important as the operating frequency moves into the 60-140 GHz region.

Having a planar structure, open microstrip line transmission medium has found wide acceptance for MIC applications in the microwave frequency region. Traditionally in this region, high purity Alumina is used as the substrate material, however, as we move into millimeter wave frequencies, problems arise with excessive dispersion and over-moding. Lower permittivity substrates (ξ_r = 2.5-4.0) are necessary to overcome these problems. Quartz substrates with ξ_r = 3.78 has been successfully used with microstrip lines up to 140 GHz.[3] Figure 9 shows the microstrip line losses on a quartz substrate with a comparison between measurements reported by Oxley[4] and Oltman[5] and calculations based on the equations presented by Gupta[6]. These results do not include losses due to radiation and surface roughness[7]. Although quartz is an attractive substrate material, it is costly, fragile and requires precision processing due to the small circuit dimen-

Fig. 8 Typical millimeter wave hybrid integrated circuit assembly.

[*Continued on page 56*]

$\epsilon_r \pm .01$ Another first from Rogers.

We've done it. Again. We've developed the lowest tolerance in dielectric constant in a microwave laminate—$\epsilon_r \pm .01$ And now you can get it. With Rogers *RT/duroid*® glass microfiber PTFE 5870, 5880.

RT/duroid with $\epsilon_r \pm .01$ The demanding designer's first choice.

RT/duroid with $\epsilon_r \pm .01$ delivers the qualities you look for in a microwave laminate. Closest control. Consistency. Precision. It's non-woven, so it has a lower dissipation factor than woven cloth structures. Its glass microfiber construction prevents wicking. *RT/duroid* far exceeds the strict standards of the military, stands up to your toughest demands.

Rogers. The leader.

For 13 years, Rogers has been first. Beginning in 1969, when we, along with the military, pioneered a practical method of measuring ϵ_r in stripline materials. Again in 1976, when we were the first to develop ϵ_r tolerance of $\pm .03$ Again in 1978, when we developed ϵ_r tolerance of $\pm .02$ And now, in 1982, with the closest control ever.

ROGERS FIRSTS	
1969	Rogers and the military develop the first practical method of measuring ϵ_r in stripline materials. Tolerance on ϵ_r was $\pm .05$
1970	Rogers reduces tolerance on ϵ_r to $\pm .04$
1976	Rogers reduces tolerance on ϵ_r to $\pm .03$
1978	Rogers reduces tolerance on ϵ_r to $\pm .02$
1982	Rogers announces tolerance on ϵ_r to $\pm .01$

Rogers application engineers. They keep us first.

Our team of application engineers make sure that when you choose Rogers *RT/duroid*, you learn how to make it work. Hard. Specify *RT/duroid*, and we follow-up with all the technical guidance and help you need. From people like Stan Keahey, a 20 year professional who can help you design successfully using the close control *RT/duroid* delivers.

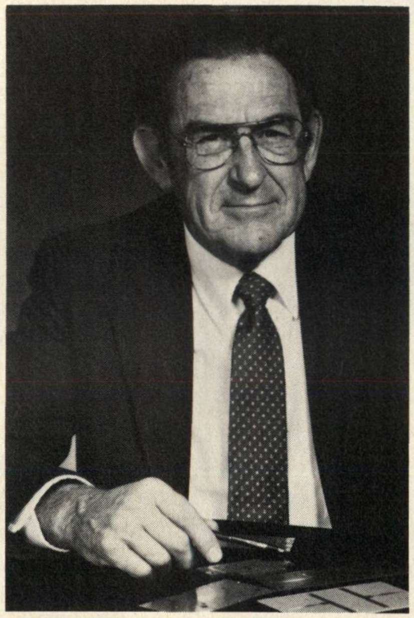

Rely on Rogers RT/duroid.

Everything you need in a microwave laminate. Closest control. Consistency. Trouble-free processing. And Rogers gives you more. Application engineers that have the same tough standards you do. Technical assistance when you need it. And the knowledge that you're doing business with a pioneer in the industry.

RT/duroid is available from precisely one company. Rogers. Ask us about it.

Call Robin Bonfield at (602) 963-4584.

ROGERS

Rogers Corporation
Chandler, Arizona 85224

CIRCLE 38 FOR IMMEDIATE NEED
CIRCLE 39 FOR INFORMATION ONLY

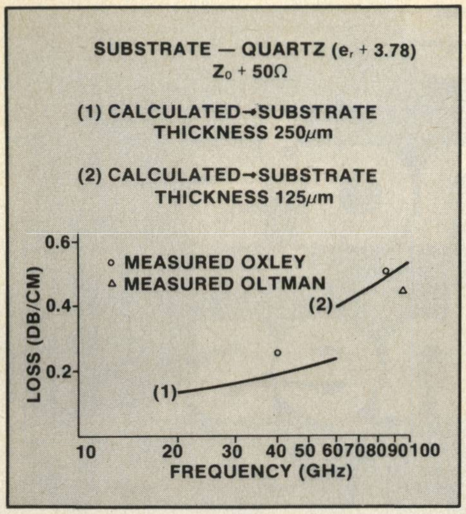

Fig. 9 Microstrip loss vs. frequency on quartz substrates.

IV. Millimeter Wave Device and Material Tradeoffs vs. Frequency

FREQUENCY COMPONENT	35 GHz	60 GHz	94 Ghz	140 GHz	MATERIALS
MIXER DIODE	Si	GaAs	GaAs	GaAs	Si - SILICON
SOURCE DIODE (CW/FMCW - GUNN)	GaAs	GaAs	GaAs/InP	InP	GaAs - GALLIUM ARSENIDE
SOURCE DIODE (PULSE - IMPATT)	Si/GaAs	Si/GaAs	Si	Si	InP—INDIUM PHOSPHIDE
VARACTOR DIODE (FMCW)	Si	Si	GaAs	GaAs	
SWITCH DIODE	Si	Si	GaAs	GaAs	
* IF AMPL. TRANSISTOR	Si BPT	Si BPT	GaAs FET	GaAs FET	

*BPT - BIPOLAR TRANSISTOR
FET - FIELD EFFECT TRANSISTOR

sions. Lower dielectric constant soft substrates such a Duriod with ε_r = 2.22 are particularly significant for low cost millimeter wave applications Figure 10 summarizes the microstrip line characteristics and key parameters for both Quartz and Duriod materials. Recent measurements carried out by Honeywell at 40 GHz and 95 GHz with two thicknesses of Duriod substrate are shown in Figure 11. It should be quite clear, particularly in W-band, that microstripline transmission losses make them unsuitable for general purpose transmission feeders. Dielectric image guide can be used to meet this need.

As shown in Table III, computer-aided design (CAD) techniques

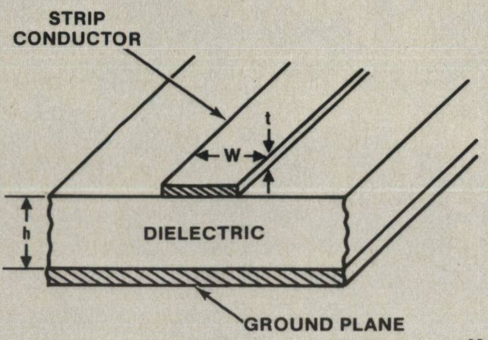

GEOMETRY
—STRIP CONDUCTOR OF WIDTH w) AND THICKNESS (t)
—DIELECTRIC SUBSTRATE OF THICKNESS (h) AND WIDTH >> (w)

LOSSES
— FOR NONMAGNETIC DIELECTRIC SUBSTRATE
—DIELECTRIC LOSS IN SUBSTRATE
—OHMIC SKIN LOSS IN STRIP CONDUCTOR

SUBSTRATES		
MATERIAL	DUROID	FUZED QUARTZ
DIELECTRIC CONSTANT	2.22	3.78
DIELECTRIC LOSS TANGENT	0.001	0.0001
MINIMUM THICKNESS (IN)	0.004	0.002
LOSS/λ(dB)	0.15	0.05
Cost ($/IN²)	0.10	4.00

Fig. 10 Considerations for microstrip at millimeter frequencies.

[Continued on page 58]

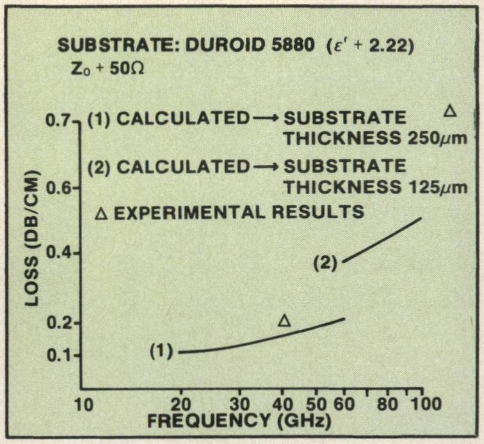

Fig. 11 Microstrip losses vs. frequency on duroid substrates.

comprising the transitions and high impedance line.[10] Numerous circuit analysis and optimization programs for 26.5 - 100 GHz have been developed by Singh.[11] Figure 12 shows the conductor pattern for a Ka-band microstrip Gunn oscillator circuit. The transmission line of length ℓ is used to tune the oscillation frequency. The Gunn diode was accurately modelled and the resulting oscillator performance predicted by CAD. From Figure 12, it is noted that there is excellent agreement between predicted and measured performance. Similarly, a microstrip balanced mixer, with conductor pattern as

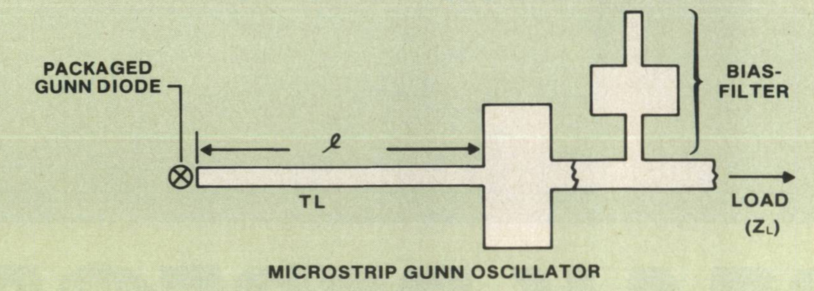

ℓ (MILS)	FREQUENCY OF OSCILLATION (GHz)	
	CALCULATED	MEASURED
105	34.0	34.4
95	35.5	35.250
88	36.75	37.15
83	37.5	37.65

Fig. 12 Design and performance of K_a-band microstrip Gunn oscillator.

are essential for performance optimization and rapid design change turn-around at millimeter wave frequencies. Numerous techniques are available in the literature to characterize one-port active devices in a waveguide configuration.[8,9] Nonetheless, these approaches are difficult to implement in a microstrip configuration and special techniques have to be devised. This consists of embedding the device at one end of a 50-ohm microstrip line, the other end of which is connected to a high quality waveguide-to-microstrip transition. The S-matrix of the whole structure is measured and the device characteristics determined by de-embedding the structure

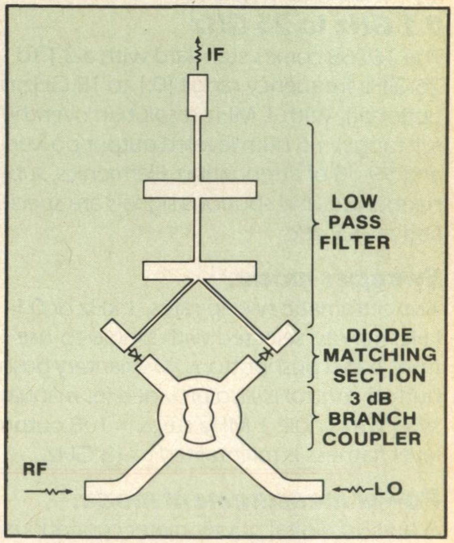

Fig.13 Typical conductor pattern for MIC balanced mixer.

[*Continued on page 62*]

[*From page 58*]

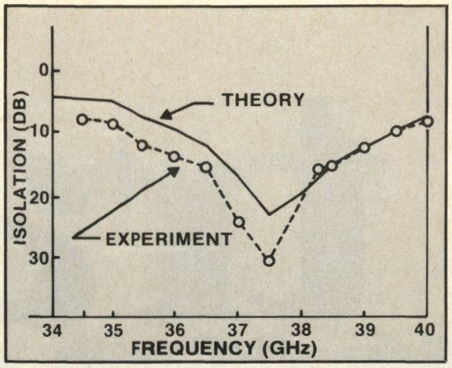

Fig. 14 Isolation vs. frequency for a K_a-band microstrip balanced mixer with GaAs mixer diodes.

in Figure 13, was modelled with CAD. The resulting agreement between predicted and measured RF to LO isolation is given in Figure 14.

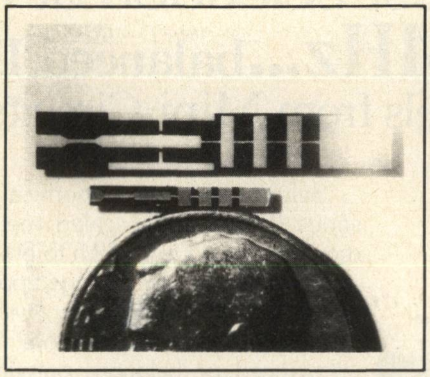

Fig. 15 GaAs monolithic mixer chips at 35 GHz and 94 GHz.

The second circuit technique for millimeter wave requirements involves monolithic GaAs processing to eventually achieve several circuit functions on a chip.[12] Ion implantation and annealing are coupled with planar fabrication technology to achieve the circuit realization. Figure 15 shows monolithic mixer chips at 35 GHz and 94 GHz as developed by Honeywell. Advantages of the monolithic mixer include very low noise figure, good isolation and excellent diode match without the time-consuming selection process necessary with hybrid MIC mixers. The FET is going to play a major role in monolithic circuitry up through 40 GHz since it has great flexibility with its three-terminal structure. Above 40 GHz, new three-terminal devices such as the permeable base transistor are being investigated with the help of molecular beam epitaxy.[13] It appears that initial monolithic circuitry at 60 GHz and 94 GHz will have to be achieved with Schottky-barrier and Gunn diode structures.

Conclusions

In summary, this paper has discussed millimeter wave component needs and options for tactical systems of the PGW class. It is clear that a new generation of components are needed in order to meet system requirements and satisfy the key factors of low cost and producibility. Initially, hybrid integrated circuit techniques are being utilized with growth to CAM for assembly and test. On the longer term, monolithic chips providing compact transmit/receive functional module capabilities are in the R&D stage with the goal of demonstrating viable millimeter wave GaAs LSIC by the end of this decade.

REFERENCES

1. Seashore, C.R., Miley J.E., and Kearns, B.A., "MM-Wave Radar and Radiometer Sensors for Guidance Systems", *Microwave Journal*, August 1979, pp. 47-51.
2. Malgeri, T.J., "Sense and Destroy Armor", *Army Research, Development and Acquisition Magazine*, November-December 1979.
3. Sissan, M.J. and Briggenshaw, P.M., "Microstrip Development at 140 GHz", Fifth International Conference on Infrared and Millimeter Waves, Wurzburg, Germany, 1980.
4. Oxley, T.H., "Millimeter Wave MIC's Rely on Hybrid-Open Microstrip", *Microwave System News*, September 1979.
5. Oltman, H.G., Weems, D.M., Lindgren, G.M. and Walton, F.D., "Microstrip Integrated Seeker Components - A Progress Report", Eigth DARPA/Tri-Service Millimeter Wave Conference, Eglin AFB, 3-5 April 1979, pp. 289-298.
6. Gupta, K.C., Garg, R. and Bahl, I.J., "Microstrip Lines and Slot Lines", ARTECH House Inc., 1979, pp. 91-93.
7. Denlinger, E.J., "Losses of Microstrip Lines", *IEEE Trans. MTT-28*, June 1980.
8. Pence, I.W. and Kahn P.J., "Broadband Equivalent Circuit Determination of Gunn Diodes", *IEEE Trans. MTT-23*, November 1970
9. deKoning, J.G., et al., "Gunn-Effect Amplifiers for Microwave Communications System in X-, K_u- and K_a-Bands", IEEE Trans, MTT-18, April 1975.
10. Penvield, P., et al., "De-embedding and Un-terminating", IEEE Trans. MTT-22, March 1974.
11. Singh, D.R., "Millimeter Wave Computer-Aided Design Programs", *Honeywell Internal Report*, December 1981.
12. Abbott, D.A., et al., "Monolithic Gallium Arsenide Circuits Show Great Promise", *Microwave System News*, August 1979.
13. Gibbons, G., "Solid State Faces New Questions", *Microwave System News*, December 1979. ■

Wideband mm-Wave Mixers For EW Applications

D. W. Ball and L. Q. Bui
Hughes Aircraft Company
Electron Dynamics Division
Torrance, California

Introduction

In parallel with the development of millimeter-wave radar weapon and communication systems, a need for millimeter-wave surveillance receivers have been increasing. Conceptual systems call for receivers capable of covering hundreds of GH_z of bandwidth. In order to meet this requirement in a manner which will be feasible from the standpoint of production costs, mixers with broadband coverage must be developed. This requires broadbandwidth capabilities at both RF and IF bands. Consequently, low parasitic, high performance mixer diodes, wide instantaneous bandwidth mixer circuits, and multi-octave low-noise IF amplifiers are needed.

This article describes the design and development of broadband millimeter-wave mixers suitable for these EW applications. Specifically covered are diode characteristics, circuit design considerations, and performance measurements over waveguide bandwidths.

The mixer design presented here yields wide instantaneous band coverage at the RF port, with selective band constraints applied to the local oscillator and input port. The IF output is band limited via low-pass and band-pass diplexing at the local oscillator/mixer diode junction. Inherent LO to RF isolation is achieved by proper use of balanced and single-ended transmission lines, along with well-matched mixer diodes.

The mixer design takes advantage of low-cost printed circuit

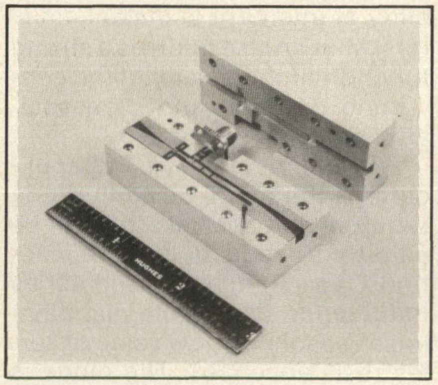

Fig. 1 Planar hybrid balanced mixer incorporating beam lead diodes.

fabrication technology which is particularly suited to batch processing and facilitates the use of low parasitic beamlead diodes. Simple circuit mounting via "split block" housing precludes the need for multiple complex machined parts, thus further reducing fabrication costs as compared to the traditional waveguide millimeter-wave mixer with whisker contacted "honeycomb" Schottky diodes.

It is worth noting that this mixer design approach leads to fully integrated multi-functional downconverters which can readily include a local oscillator, low noise amplifier, antenna, appropriate preselection and post-selection filters, or other integrated circuitry which complement the downconverter assembly. Integrated receivers using monolithic or millimeter-wave integrated circuitry are under particular scrutiny due to their inherent small size and low production cost. This benefit offers considerable advantages when mechanizing multi-channel receivers for applications where space is a premium.

EW Mixer Design Considerations

The EW mixer specifications require exceptional solutions to opposing performance criteria.

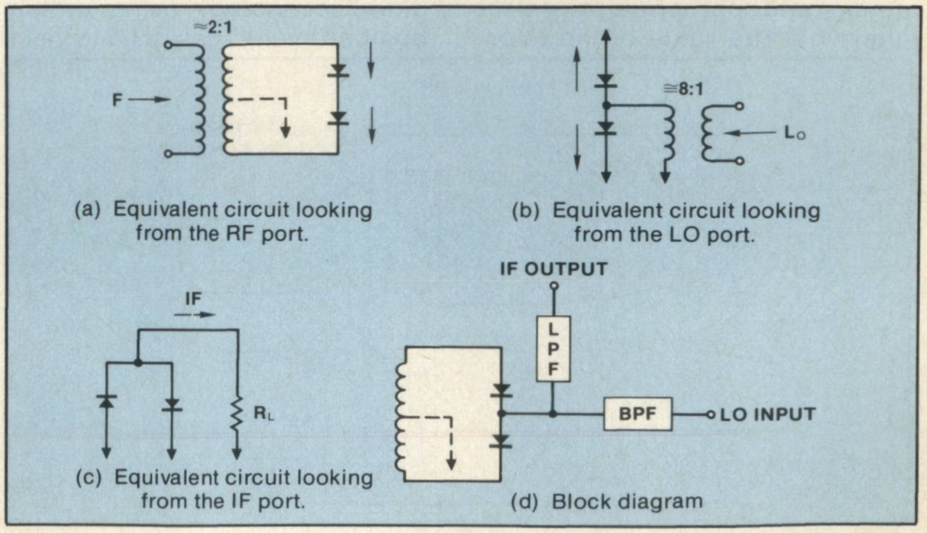

Fig. 2 Singly balanced mixer

Typical receiver trade-offs are geared around the following requirements:

- High spurious-free dynamic range
- Flat, low-noise figure response
- Full waveguide band or greater frequency coverage
- Small size and low cost

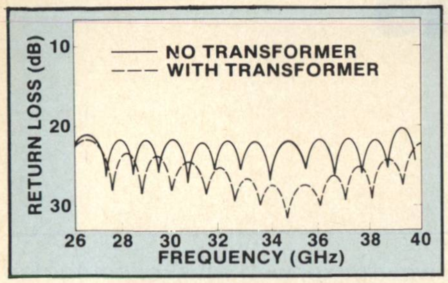

Fig. 3 Return loss comparison of matched vs. unmatched interface of the waveguide to slot transition.

Generally, EW receivers are required to process multiple emitters in a relatively dense spectral environment. Intermodulation products, single tone or multitone, generated internally or externally to the receiver are the limiters of dynamic range. They can result in false emitter detection and effectively desensitize the receiver.

To the first order, the degree of linearity of the receiver is defined by the mixer/IF amplifier single-tone and two-tone intermodulation intercept point. The higher the intercept point the higher the spurious free dynamic range. (It should also be noted that some intermods are level independant and can only be reduced by proper choice of local oscillator frequency and appropriate pre-select filtering). The value of the intercept point for the mixer is determined by a number of conditions under the control of the designer, they are:

- Mixer type (single-ended, balanced, double balanced)
- Available local oscillator power
- Mixer diode choice
- RF/LO/IF network matching circuitry.

The effects of each option noted above must be taken into consideration in terms of impedance levels and parasitics to insure wideband flat mixer response. Contrasted with dynamic range, the mixer must also provide a low noise figure to insure the probability of intercept of distant emitters. Mixer noise figure is a strong function of the quality of the converting diode(s) and its associated parasitic elements.

For millimeter-wave EW applications the diode design criteria requires that special attention be paid to the reduction of the junction Capacitance (C_j) and series inductance (L_s), while maintaining a reasonably low value of series resistance (R_s). The diode is designed to maintain a high barrier potential via appropriately selected Schottky metal so as to allow strong local oscillator drive for high intercepts without sacrificing bandwidth or noise figure.

A number of diode configurations are available. Whisker contacted diodes have shown the lowest spot noise figures reported to date[1]. The beamlead diode using mesa-etch technology is fast catching up[2,3]. Advanced planar diode technology using proton bombardment [4] designed to yield a truely planar device is being developed with the ultimate goal of growing arrays in-situ, so that, stray parasitic inductances are virtually eliminated. It should be noted that, contrary to popular beliefs, whisker contacted mixers do withstand the severe environmental conditions of space and military qualifications tests since the whiskers mass is extremely small. The main drawback associated with the whisker contacted diode is that the series inductance and post-mount capacitance, as viewed from the RF and IF port severely limit the bandwidth performance of the mixer. In addition, the assembly of whisker contacted mixers is labor intensive thus costly. For EW applications, IF frequencies in some cases extend to Ka-band and above. The beamlead diode junction capacitance typically runs 2 to 3 times that of the 2 micron dot whisker contacted device. However, the planar diode, when mounted in an appropriate structure yields a comparatively small series inductance. This results in the junction capacitance to be essentially de-embedded, thus it can be theoretically cancelled using external matching elements.

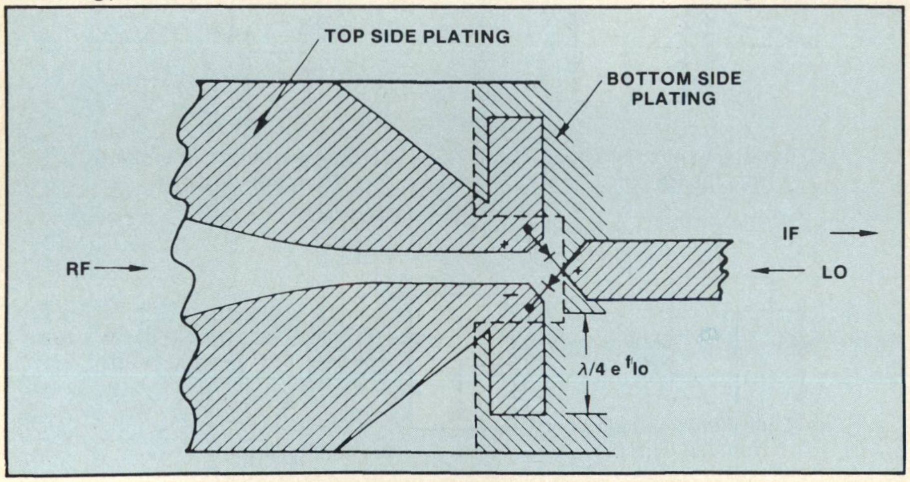

Fig. 4 Diode location on planar hybrid mixer.

Although planar circuit designs are inherently broadband, it is mandatory that high efficiency waveguide to other media transitions be developed. It is important that a number of variations be available to accommodate special mechanical configuration needs. A few key transitions are listed below:

- Waveguide to dielectrically loaded crossbar
- Waveguide to slot transition
- Probe-coupled transition
- Waveguide to microstrip transition

Since planar circuit dielectric and conductor losses can be appreciable at millimeter-waves, the mixer designer must selectively distribute these losses so as to maximize the key mixer performance parameters. This is done in conjunction with maintaining a simple low-cost housing structure. Ideally, the converting diodes are mounted as close to the RF port as possible so as to

[Continued on page 68]

[From page 66]

minimize path losses which add directly to noise figure. Losses due to LO injection are not as critical, but must be attended to since LO power at millimeter-wave frequencies comes at a premium. For this reason, the planar circuit mixer reported here is hybrid by nature, in that various propagation media are used to optimize performance.

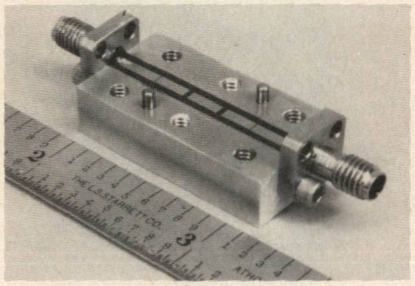

Fig. 5a Prototype local oscillator band pass filter.

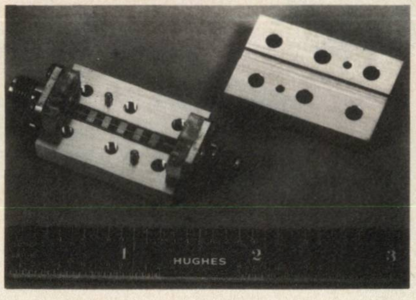

Fig. 5b Prototype IF low pass filter.

Hybrid Mixer Design

This mixer has been developed for use at K and Ka-band. The mixer is singly balanced and uses beamlead diodes mounted on a low dielectric constant substrate material.

A photograph of the mixer is shown in Figure 1. A block diagram of the mixer and its circuit elements are shown in Figure 2. The "hybrid" mixer is so called because three propagation media are used. The RF input uses a wave-guide to slotline transition centrally located in the waveguide to yield a wideband balanced line transformer which is terminated by a matched diode pair. The transition uses a cosine taper whose length is 2λ at the center frequency of Ka-band. Figure 2a shows the simplified equivalent circuit as seen from the RF port. The slot impedance was chosen to be 200 ohms which is consistent with two diodes in series at a nominal pump power of +10 dBm. The cosine taper was evaluated for electrical lengths of 1, 2 and 3 wavelengths over the full waveguide bandwidth. It is interesting to note that the return loss for all these transitions got progressively better, but not dramatically, with added length, starting at 18 dB for the 1λ case and limiting to 23 dB for the 3λ case. The 23 dB limit is attributed to the waveguide-to dielectrically loaded waveguide interface. Figure 3 shows this indeed was the case, where a matching transformer was added at the interface and provided a band-limited improvement of the return loss.

Unlike the RF port, the local oscillator is injected into the diode pair using a single-ended transmission line. Figure 2b shows the equivalent circuit as viewed from that node. The problem here is to provide a good LO return so that the diodes are well biased. This is accomplished by adding open shut stubs at on the balanced input as shown in Figure 4. The lengths of the stubs may be trimmed to optimize the LO match by observing the return loss on a reflectometer test setup.

The LO is transitioned from waveguide to microstrip and then to suspended microstripline to accommodate a low-loss, 3 pole, 0.1 dB ripple, Tchebychev filter, using end-coupled resonators. This filter type is particularly suited for fixed LO mixers. The structure facilitates fringing capacitance analysis, thus simplifies the design procedure. Figure 5 shows a photograph of the prototype filter. Figure 6 illustrates the filter response, indicating good in-band loss characteristics (<1 dB α30 GHz).

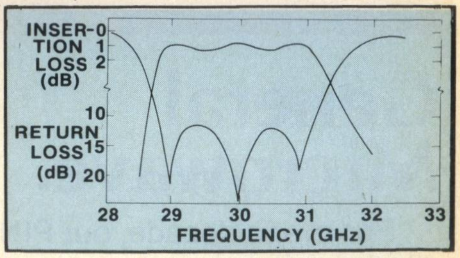

Fig. 6 Prototype filter frequency response.

The waveguide to microstrip transition uses two overlapping cosine tapers by way of two-sided

[Continued on page 72]

substrate etching. This circuit provides a simple in-line technique for converting to the microstrip propagation mode and is very broadband. As with the waveguide to slot transition, this circuit was evaluated at electrical lengths ranging from 1 to 3 wavelengths. Test results showed that 2 wavelengths yielded 18 dB return loss, which was adequate for this application. This transition is particularly sensitive to, symetrical location in the H-plane of the wave-guide for tapper lengths of 1 and 2 wavelengths. This is attributed to extraneous modes being generated due to the assimetry in the transition region. It was noted that the sensitivity lessened as the transition was lengthened.

The IF frequency is picked off using a five-section low-pass filter designed in microstripline. Distributed lines were used to approximate lumped elements. The series elements (l's) used high impedance lines (130 Ohms), whereas the shunt elements (C's) were approximated by using open shunt stubs whose lengths where chosen to be quarter-lamda at the LO frequency. The impedance of the stubs were commensurate with the net capacitance required for each unit element of the filter. The total network analysis includes the parasitic capacitance of the diodes (Figure 2c). As with LO filter, the low pass structure was optimized for flat response to 18 GHz with high insertion loss in the 26 to 30 GHz range. Since the LO filter and IF filter are in parallel, the problem reduces to a simple diplexer and should be analyzed together. This procedure insures against extraneous loading of one filter with the other.

Fabrication

As seen in Figure 1, the housing is a simple split block design, which was fabricated using a numerically controlled end-mill. Note that the mixer consists of six parts, including the diodes, which is consistant with low cost fabrication techniques.

The two-sided printed circuit was layed out and the rubylith cut using a desk top calculator (HP9825) and plotter (HP9872B). The plotter pen was modified so that a special blade could be inserted, thus enabling the use of standard graphics subroutines to modify or cut new rubyliths. The fabrication feature allowed a number of quick iterations and variations to be tried and evaluated in a short period of time.

The substrate material used was 10 mil thick Duroid® with half-ounce copper plating. Line widths and gaps were limited to 4 mils and taken into account early in the design stage so that processing yield may be maximized.

The beamlead diodes were soldered to the substrate using Indium® solder whose liquid state was 140° C.

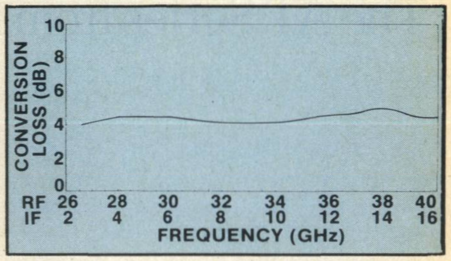

Fig. 7 Conversion loss of hybrid mixer.

Hybrid Mixer Test Results

The mixer was evaluated for RF coverage from 26 GHz to 40 GHz at a fixed LO of 24 GHz. LO drive was +10 dBm. The IF band was evaluated to 16 GHz although good response is expected to extend to 18 GHz. Figure 7 shows the wideband response of the mixer at both RF and IF ports. The conversion loss ranged from 4 to 5.2 dB over the 14 GHz IF bandwidth. Subsequent experiments resulted in conversion losses as low as 4.5 dB over narrow bands (3-5 GHz) by incorporating a quarter-wave

TABLE I
HYBRID MIXER SPECIFICATIONS

RF Band	26 - 40 GHz
LO Frequency	24 GHz fixed
IF Band	2 - 16 GHz
Conversion Loss	4.6 dB ±.5 dB
Input VSWR	
RF Port	2.0:1 max
LO Port	2.0:1 max
Output VSWR	
IF Port	2.0:1 max
LO Power	+10 dBm max
3rd Order Intercept	+20 dBm

[Continued on page 76]

length matching section appropriately located in the slot transition preceding the diode pair. Table 1 summarizes the mixer specifications.

Conclusions

The hybird mixer described in this paper offers a considerable performance improvement over whisker-contacted mixers in terms of instantaneous bandwidth at the RF and IF ports. A major result of this mixer development is that cost savings are incurred by parts reduction and improved fabrication procedures. As a result, the mixer can be used in multichannel receivers, yet maintain overall systems cost at a reasonable level. The mixer topology lends itself to intergration with other planar structures that results in further reduction in both overall size and production cost.

Acknowledgements

The authors wish to thank Ms. Y. Weyand for fabrication of the mixer. ■

REFERENCES

1. Begemann, G., *"An X-Band Balanced Finline Mixer"*, Presented at the 1978 IEEE MTT-S International Microwave Symposium.
2. Cohen, S., *"Parallel-Coupled Transmission Line Resonator Filters"*, IEE Trans, Vol MTT-11, pp 223-231, 1958
3. Reindel, J., *"Mixers Simplify Millimeter Surveillance"*, MSN, Vol 10, pp 71-74, August 1980
4. Cardiosmenos, A. G., *"Planar Devices Make Production Practical"*, MSN, Vol 9, pp 46-56, May, 1979

Advanced Components for mm-Wave Systems

P. J. Meier, S. Nussbaum, J. A. Calviello, L. D. Cohen, H. Levy, J. Levy, N. Arnoldo, and P.R. Bie
Eaton Corporation AIL Division
Melville, NY

Introduction

Recent advances in component technology have provided performance/cost benefits for a new generation of millimeter-wave systems. System applications sharing in these benefits include surveillance, tracking, guidance, communication, atmospheric study, and radio astronomy. Better performance and/or lower cost can be achieved with advanced components including filters, couplers, mixers, oscillators, and switches. This paper describes recently developed millimeter-wave components constructed by various techniques such as hybrid IC, monolithic IC, and conventional waveguide. Each approach is tailored to a specific combination of system requirements in terms of performance specifications, cost (development and manufacturing), and the anticipated production volume. The examples to be described include E-plane and H-plane components (for moderate production volume), a monolithic mixer (for potentially large production runs), and waveguide components (for those applications where performance is more important than cost).

E-Plane and H-Plane Components

A wide variety of millimeter-wave components have been developed by embedding a hybrid IC or an etched metallic circuit in the E-plane or H-plane of a split-block housing.[1-3] The approach offers printed-circuit economy in both the developmental and production phases of a moderate-volume program. The artwork and masks can be prepared quickly, and printing tolerances can be held to ±0.0005 inch with common chemical-etching equipment. In many circuits, fin loading places the waveguide housing far from cutoff, thereby allowing looser tolerances than those applicable to the inner walls of conventional waveguide. Typical values of the unloaded Q achieved at Ka-band are 1500 for metallic E-plane filters[4] and 300 to 700 for fin-line (with heavy to light loading). This range of unloaded Q values falls between the limits of 120 for microstrip circuits[5] and 5000 for conventional waveguides.[6]

Figure 1 shows a variety of E-

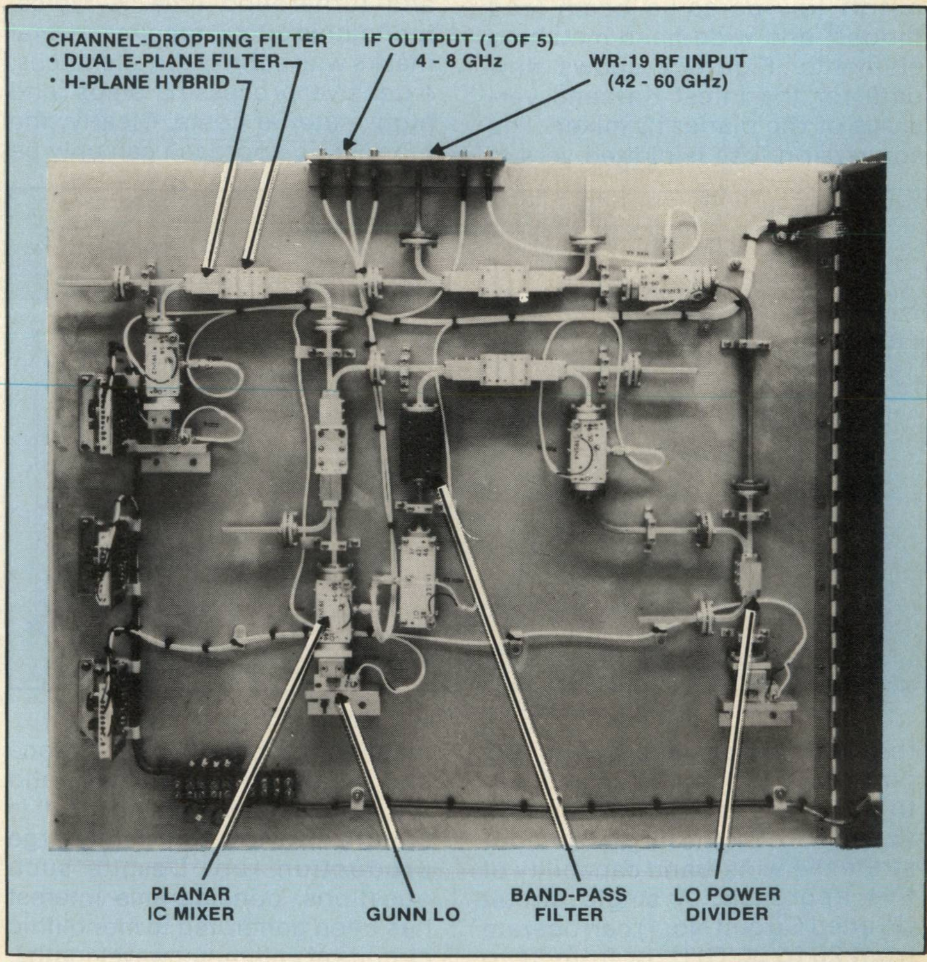

Fig. 1 E-plane and H-plane components in channelized receiver.

plane and H-plane components interconnected to form a breadboard channelized receiver. RF signals in the band of 42 to 60 GHz enter at a WR-19 port and are sorted into five contiguous channels by a bank of channel-dropping filters. Each channel-dropping filter contains a dual E-plane filter embedded between H-plane hybrids. Because the channel-dropping filters are matched at all ports, they can be cascaded with negligible interaction. The loss is typically 3 dB over a 4-GHz passband in each channel of the WR-19 system; the loss can be as low as 1 dB for a Ka-band system.[4] A 7-pole 0.1 dB Tchebycheff response provides a 45 dB rejection bandwidth of 8 GHz.

Other key components in the illustrated system are the planar IC mixers. Each mixer integrates fin-line, coplanar line, and microstrip on a single substrate.[7] The design has been recently refined by incorporating high-cutoff low-parasitic beam-lead diodes[8] and wide-band matching elements. Figure 2 shows new data for the latest Ka-band versions of the planar IC mixer. The conversion loss is plotted versus the signal frequency, with LO power as a parameter. In addition to achieving low conversion loss (5.0 to 65. dB), the mixers demonstrate the wide-band capability of this approach. A single circuit (Printed Circuit No. 1) can operate from 26 to 30 GHz, or from 34 to 38 GHz, with the LO fixed at 32 GHz. Work is now in progress to wide band the IF circuit and thereby cover a full waveguide band with a single printed-circuit mixer. By increasing the bandwidth of each channel, fewer channels will be required and the system can be improved in terms of size, weight, and cost.

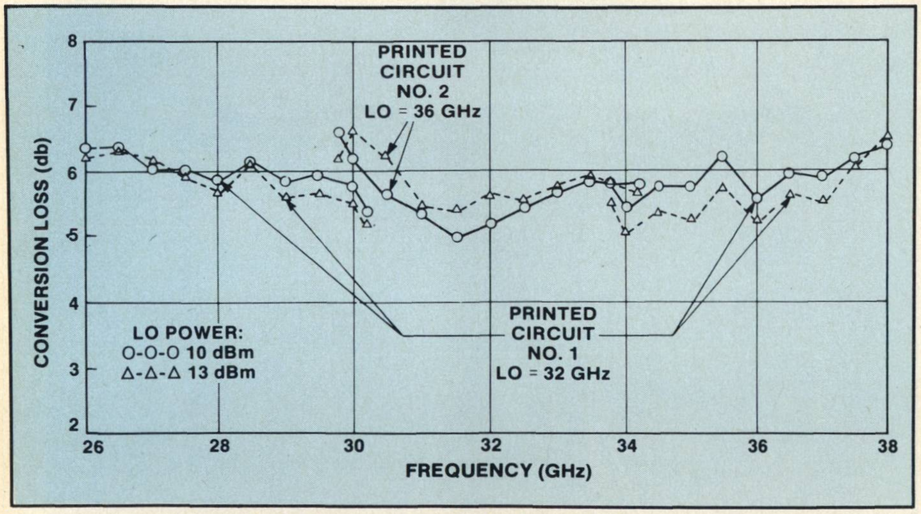

Fig. 2 Conversionloss of planar IC mixers.

Monolithic IC Mixer

Although millimeter-wave systems have so far been constructed in small or moderate quantities, certain appliations for large-volume production have been identified. Suitable applications include phased-array modules, radio-metric seekers, and anti-collision radars.

The monolithic approach can reduce the unit cost, but not without penalties. Monolithic circuits generally use microstrip, which has Q limitations.[5] Although the total loss can be minimized by closely integrating the circuit elements, fundamental limits are imposed by stray coupling. Other penalties are the development cost and turnaround time. A typical monolithic circuit requires several masks with submicron tolerances, extensive processing steps, and high material costs. Clearly, the monolithic approach can only be justified if adequate performance and yield can be achieved, and the added development cost is amortized over a sufficiently large production run. Despite such questions, considerable interest has been generated in monolithic circuits at millimeter wavelengths. This interest is well deserved, given the potential capability to fabricate dozens of receivers from a single wafer, without costly hybrid bonding operations.

As a first step toward the development of a Ka-band monolithic mixer, we have integrated the required microstrip circuit elements on a semi-insulating GaAs substrate measuring 5 by 140 by 180 mils. Figure 3 shows the breadboard circuit which includes a single-section branch-line hybrid, diodes mounts, and an IF-output filter. At the present stage of development, the mixer is termed quasimonolithic, as beam-lead diodes have been bonded to the GaAs circuit. This circuit, and other circuits containing isolated elements such as the hybrid, were fabricated and tested to confirm the microstrip dimensions prior to a fully monolithic demonstration.

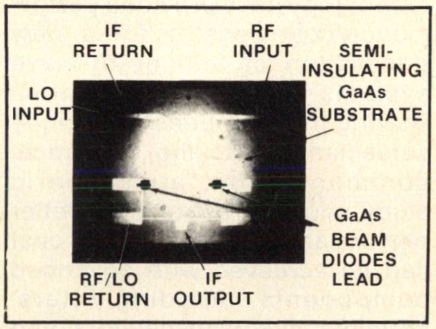

Fig. 3 Ka-band balanced mixer on semi-insulating GaAs.

The quasimonolithic mixer was tested by embedding the GaAs circuit between low-reflection microstrip/waveguide transitions at the RF and LO ports. The IF was extracted through a short length of semirigid coax and an SMA connector. Figure 4 shows the measured conversion loss of the mixer versus the signal frequency, with the LO frequency as a parameter.

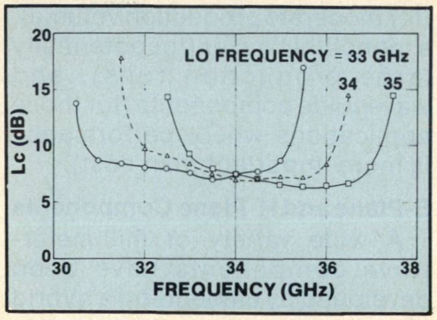

Fig. 4 Conversion loss of quasimonolithic mixer.

[Continued on page 84]

With the LO fixed at 35 GHz, the conversion loss varies from 6.2 to 7.5 dB across the RF band of 34 to 37 GHz. The plot also shows that the RF band can be shifted lower by step-tuning the LO to 33 or 34 GHz. The results were obtained with an LO drive level of 16 dBm. With the drive reduced to 13 dBm, the conversion loss is typically 0.2 dB higher.

Work is now in progress on the development of a fully monolithic Ka-band mixer containing the previously tested microstrip elements. Through parallel programs, the relative merits of a planar approach (utilizing proton) bombardment) and a mesa approach will be studied. The objective is the development of a mixer front end (and eventually an entire receiver) applicable to a new generation of low-cost millimeterwave systems.

Waveguide Components

Despite the current interest in hybrid and monolithic circuits, there is a continuing need for high-performance components constructed in conventional waveguide. The unloaded Q of the waveguide approach remains unrivaled among shielded, single-mode transmission lines.[6] The lower loss afforded by this approach is still justified in critical applications, particularly when the production volume is modest.

Examples of recently developed waveguide components are described in the following paragraphs. The examples include a low-loss ferrite switch, a cavity-stabilized Gunn oscillator, and ultra-low-noise mixers.

— Ferrite Switch

Although excellent results have been achieved with solid-state switches at millimeter wavelengths, there are applications where holding power is not available. If additional requirements (such as operating life or reliability) rule out mechanically latching switches, a ferrite approach is required.

Figure 5 shows a recently developed, latching, Ka-band, low-loss, high-isolation switch. The component is basically an H-plane latching circulator with one port internally terminated to form an SPST switch. The latching element is a lithium ferrite with a saturation magnetization of 5000 gauss. The ferrite is matched to each waveguide port with a ceramic vane whose dielectric constant is 6. The performance of the switch is summarized in Figure 6. Across the band of 32 to 37 GHz, the insertion loss is less than 0.25 dB and the isolation is 25 to 34 dB. The measured switching speed is less than 3 μsec.

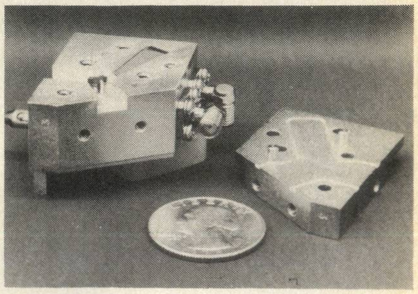

Fig. 5 Latching ferrite switch.

Because of the low per pass, it should be feasible to interconnect SPDT versions of this switch to form a multithrow switch. Such multithrow switches would be applicable to step-scanned receivers and multibeam systems.

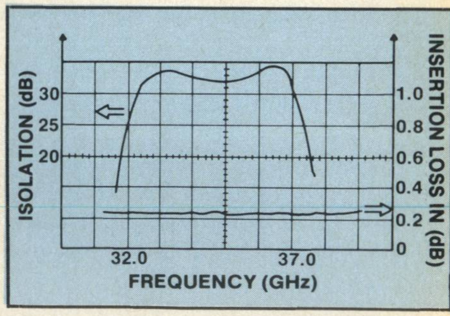

Fig. 6 Performance of latching ferrite switch.

— Cavity-Stabilized Oscillators

Another component well-suited to waveguide construction is the cavity-stabilized local oscillator. Figure 7 shows a lumped-element Ka-band oscillator which is stabilized by a copper-clad Invar-36 rectangular waveguide cavity. The component is similar to a previously described oscillator[4], except that a TE-102 transmission cavity is utilized rather than a reaction cavity.

The measured transmission loss of the cavity was 2.6 dB. The

[Continued on page 86]

[*From page 84*] **COMPONENTS**

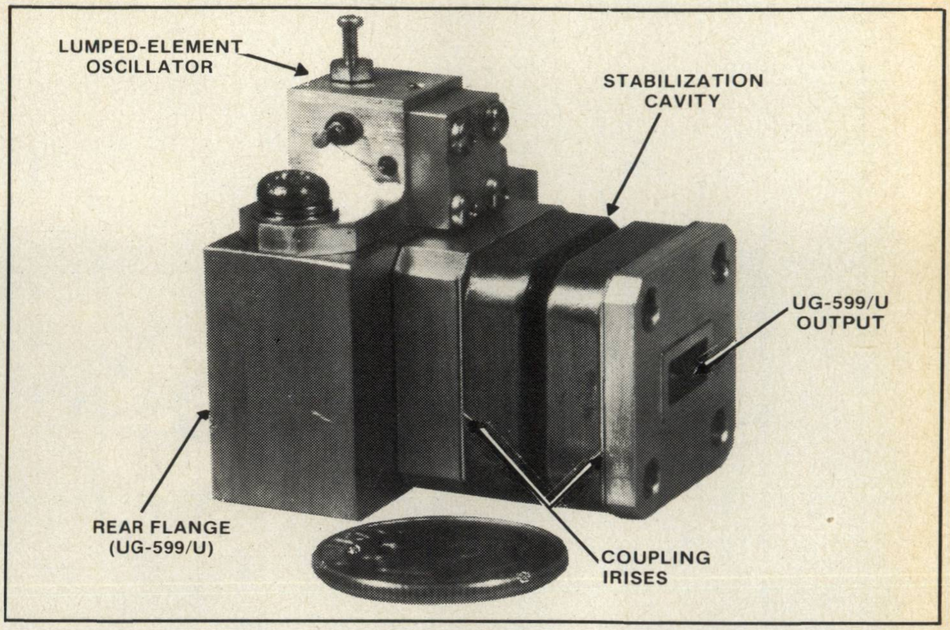

Fig. 7 Gunn oscillator with transmission cavity stabilizer.

stabilized oscillator exhibited a stabilization factor[9] of approximately 5 as determined from the ratio of measured oscillator free-running and stabilized frequency/temperature performance. A comparable stabilization factor was obtained from oscillator pushing data. The output power was 20 mw at 34 GHz and the power/temperature sensitivity was 0.028 dB/°C. Measurements and calculations showed that a stability of -110kHz/°C is feasible.

An interesting aspect of the work with the transmission cavity was that the short-circuit back plate and damping resistance at the rear waveguide output port of the oscillator could be removed, and the oscillator could be used to supply stabilized outputs to dual loads. The unit provided dual stabilized outputs without the penalty of the size and cost of directional coupler. In addition, an RF damping resistor, normally used with a transmission-type stabilizer, was not required with the two-port arrangements.

— Ultra-Low-Noise Mixers

The waveguide approach is well-suited to receivers for radio astronomies, where the ultimate in low-noise performance is required. Recently, a series of ultra-low-noise mixers covering the RF bands of 35 to 50 GHz, 70 to 90 GHz, and 90 to 120 GHz have been developed.[10]

Figure 8 shows the biphase mount utilized in the mixers. The beam-lead diodes[8] are mounted, anode to anode, on a quartz substrate mounted in the E-plane of a reduced-height waveguide. The mount is reactively terminated by a tunable waveguide back-short. The RF and LO, which enter from a single port, are diplexed by a waveguide ring filter.[11] The IF is extracted through an H-plane contact as shown.

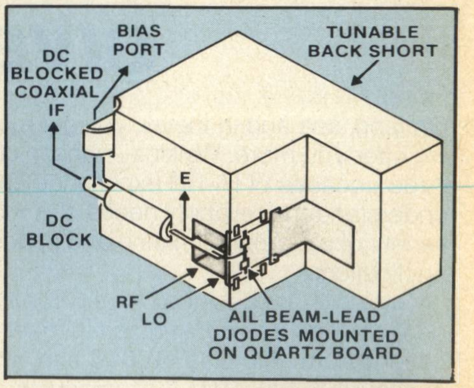

Fig. 8 Biphase mixer configuration.

This type of mixer configuration has the following advantages:

- Natural isolation between RF and IF port
- Natural isolation between LO and IF port
- Waveguide RF circuit fabricated through a hobbing technique that is not only cost-effective, but results in a better than 8-μ inch finish.
- RF impedance is favorable for

[*Continued on page 88*]

TABLE I

Freq (GHz)	Conversion Loss (dB) @300°K	@77°K	@20°K	SSB Mixer Noise Temp (K) @300°K	@77K	@20°K
35	4.0		3.7	336		115
60	4.5	4.2		490	260	
94	4.5			440		
110	5.2			670		

wide-band performance because the two diodes are in series across the guide.

- IF impedance is favorable for wide-band performance because the two diodes are in parellel across the IF transition line.
- Bias can be easily applied from a uniploar supply to reduce the LO power requirement to less than 1 mw.

The measured performance of the mixers, at ambient temperatures of 300, 77, and 20 K is summarized in Table I.

By combining a high-Q waveguide approach with low-parasitic beam-lead diodes, the insertion loss has been minimized and a wide-band, rugged, whisker-free assembly has been produced.

Conclusion

This paper describes advanced millimeter-wave components which are constructed by various techniques including hybrid IC, monolithic IC, and conventional waveguide. The relative merits of each approach are discussed with regard to performance, cost, and volume. The components described are planar and hybrid IC's (for moderate production volume), a monolithic mixer (for potentially large production runs), and waveguide components (for particularly demanding requirements). By selecting the correct approach for a given application, the technical and economic objectives can best be satisfied. As advanced components (with enhanced performance/cost benefits) become more readily available, a new generation of millimeter-wave systems can become a reality.

Acknowledgments

The channelized-receiver components were developed for NOSC under the direction of J. E. Reindel and the waveguide mixers were developed for the Tokyo Astronomical Observatory, represented by Professor M. Morimoto. The work was performed at Eaton Corporation AIL Division, Advanced Technology Systems, which is directed by B. J. Peyton. The component and device development was directed by J. J. Whelehan and J. J. Taub. Project supervisors included S. Becker, G. Irvin, S. W. Fung, and F. P. Parini. Technical assistance was provided by A. Cooley, A. Kunze, J. Pieper, and A. Reese all from the AIL Division. ■

REFERENCES

1. Meier, P.J. "Millimeter Integrated Circuits Suspended in the E-Plane of Rectangular Waveguide," IEEE Trans, Vol MTT-26, p 726-733, October 1978.
2 Reindel, J. "Printed WG Circuits Trim Component Costs," Microwaves, p 60-63, October 1980.
3. Bates, R. N. et al, "E-Planes Drop Millimeter Costs," Microwave Systems News, p 74-80, December 1980.
4. Meier, P. J., K. D. Breuer, L. D. Cohen, N. Worontzoff, J. Lepore, and J. Gunther, "Channelized Receiver Covering 26 to 60 GHz with Planar Integrated-Circuit Components," Digest of IEEE MTT-S Symposium, p 411-413, June 1981.
5. Gopinath, A., "Maximum Q-Factor of Microstrip Resonators," IEEE Trans, Vol MTT-29, p 128-131, February 1981.
6. Tischer, F. J., "Experimental Attenuation of Rectangular Waveguides at Millimeter Wavelengths," IEEE Trans, Vol MTT-27, p 31-37, January 1979.
7. Meier, P. J., "4 and 5 mm Band Printed Circuit Balanced Mixers," Microwave Journal, p 66-68, August 1979.
8. Calviello, J. A., S. Nussbaum, and P. R. Bie, "High-Performance GaAs Beam-Lead Mixer Diodes for Millimeter and Submillimeter Applications," Digest of IEEE ED Meeting, p 692-695, December 1981.
9. Ashley, J. and C. Searles, "Microwave Oscillator Noise Reduction by a Transmission Stabilizing Cavity," IEEE Trans, Vol MTT-16, p 743-748, September 1968.
10. Nussbaum, S., J. 'A. Calviello, E. Sard, and N. Arnoldo, "Widely Tunable Millimeter-Wave Mixers Using Beam-Lead Diodes," IEEE MTT-S Symposium, Dallas, Texas, June 1982.
11. Cong, H., A. R. Kerr, and A. J. Mattauch, "The Low-Noise 115-GHz Receiver on the Columbia G1SS 4 Ft. Radio Telescope," IEEE Trans, Vol MTT-27, p 245-248, March 1979.

GaAs FET Technology: A Viable Approach to Millimeter-Waves

H. Yamasaki
Torrance Research Center,
Hughes Aircraft Company
Torrance, California

Introduction

The original idea of the field effect transisitor was proposed by Schottky in 1952[1], and implementation of this idea began with silicon and then later with GaAs. The first realization of the Schottky barrier gate GaAs FET was reported twelve years ago[2]. Since then, the performance of GaAs FETs has been improving significantly every year in terms of noise figure, output power and operating frequency. They have already established a solid basis in microwave systems. A few years ago the frequency of FET operation reached upper Ka-band[3, 4] for the first time, and more recently progress of the FET has established this device firmly in the lower portion of the millimeter wave field. A 70 GHz FET oscillator[5] and a 40 GHz high gain lower noise amplifier[6] have presented strong evidence that the FET will soon become a viable millimeter-wave device. Considering the present rate of progress in the field, it is expected that the FET operating frequency will soon reach 94 GHz. Monolithic integration of the GaAs FET into microwave circuits (ICs) fabricated on a GaAs substrate has gained significant attention from both the microwave system as well as the device communities because monolithic circuits may offer significant cost reduction as compared with hybrid circuits. In the millimeter-wave region, however, the monolithic circuit is expected to achieve improved RF performance in addition to the

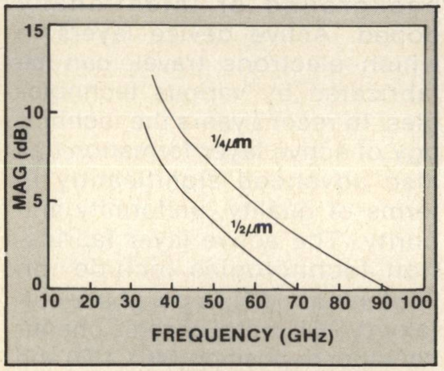

Fig. 1 A comparison of the computed gain of ½ μm and ¼ μm devices

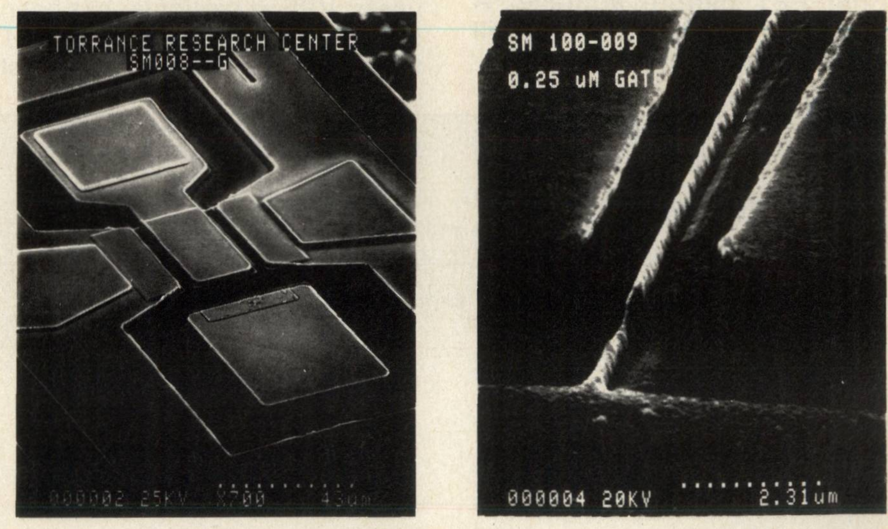

Fig. 2. SEM photograph of 0.25 x 80 μm MESFET and magnified view of No. 0.25 μm gate.

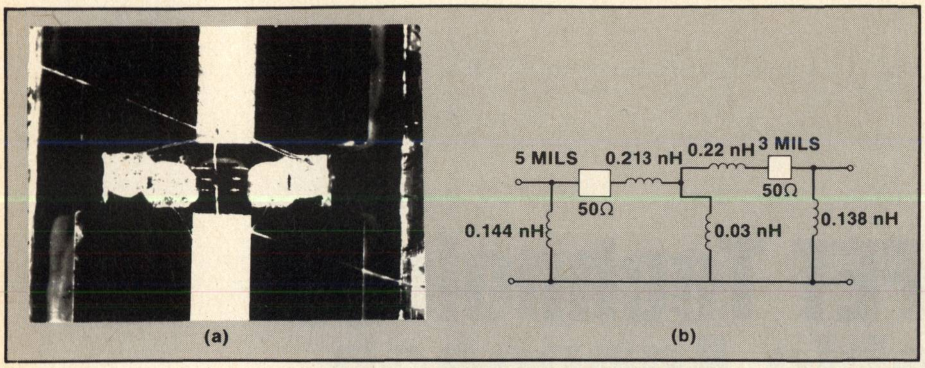

Fig. 3. A photographic view of prematched amplifier (a) and the equivalent circuit (b).

possibility of cost reduction. Therefore, monolithic integration of FETs and millimeter-wave circuits is very attractive. For example, workers at MIT Lincoln Laboratory[7] recently reported a 31 GHz monolithic GaAs heterodyne receiver chip using planar Schottky barrier diodes as a balanced mixer and a FET as a 2 GHz IF amplifier. This approach may be feasible for extending the mixer frequency to 200 GHz and the frequency of the FET IF amplifier to 60 GHz.

This paper will describe the present status of GaAs FET technology including materials, low noise and power discrete FETs, and monolithic ICs operating in the lower portion of the millimeter spectrum. The limitations of the FET in the millimeter-wave region will also be discussed. New FET-like devices currently under development may eventually reach frequencies which the conventional FET cannot achieve. A number of such new devices will be described.

GaAs Materials

It is certain that the progress achieved in GaAs materials technology has made a significant contribution to the recent advancements in FET performance. GaAs crystals, unlike silicon, can provide high resistivity substrates. Such substrates include numerous impurities which are either background or intentionally doped. Active device layers in which electrons travel, can be fabricated by various technologies. In recent years the technology of active layer formation has also advanced significantly in terms of quality, uniformity and purity. The active layer fabrication technologies include ion implantation (II), vapor phase epitaxy (VPE), metal organic chemical vapor deposition(MOCVD) and molecular beam eptitaxy MMBE. The first two technologies have been used for FET material fabrication for many years, VPE in particular has been used since the beginning of FET technology development. The last two material technologies are relatively new. Technology based on MBE may offer substantially advanced materials when it is further developed because of excellent control of material growth. It is capable of growing pure films as thin as 50 A with very sharp transitions between layers. This will be a material technology of the future and will likely be very important in the fabrication of millimeter-wave FETs.

Materials technology based on VPE has consistently provided high quality active layers for FETs. This material continues to improve in terms of uniformity in thickness and doping density. At the present time, the VPE material is the only viable source for millimeter wave FETs. The device results described in this paper were all obtained with FETs made from VPE.

Millimeter-Wave MESFETs

A figure-of-merit useful for evaluating the high frequency capability of the FET is the cut-off frequency, f_T. This parameter can be approximated by $f_T = g_m/2\pi\ C_{gs}$, where g_m and C_{gs} are transconductance and source to gate (input) capacitance, respectively. This formula suggests that increasing g_m and/or decreasing C_{gs} will improve f_T. The values of these device parameters relate to the material properties as well as the geometrical parameters of the FET. The approximate cutoff fre-

TABLE I

Noise Figure and Gain Measured from MESFETs with 0.25-0.3 μm gate length

Freq. (GHz)	Noise Figure (dB)	Ass. Gain (dB)	MAG (dB)	Company
18	1.9	7	11	Toshiba
	2.1	9	—	Plessey
27	3.6	5	—	Plessey
29	3.7	6.9	—	Hughes
30	4.0	5	8	Toshiba
38	5.5	7	10	Hughes
40	—	—	4	Plessey

[*Continued on page 96*]

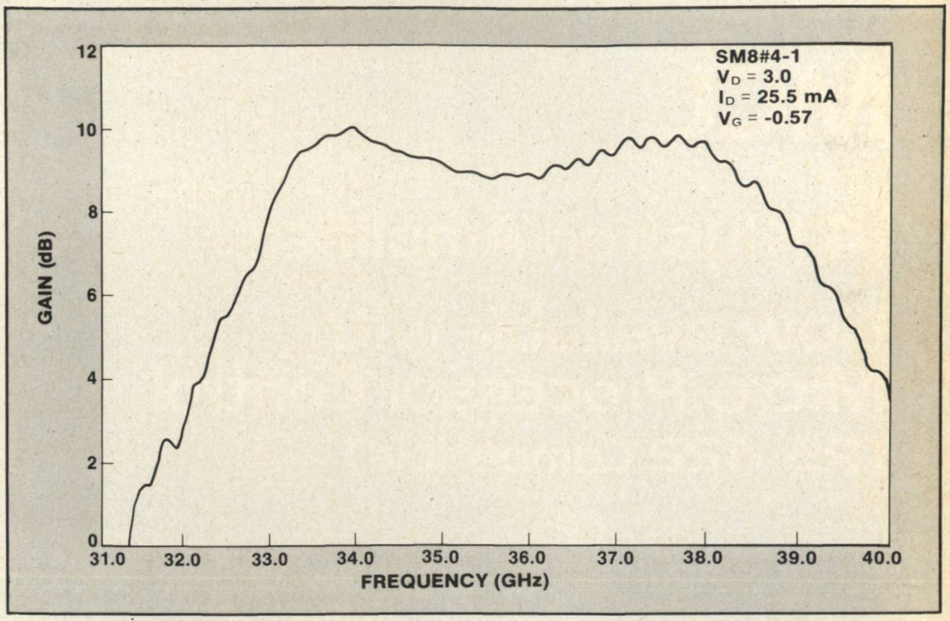

Fig. 4. A 40 GHz single stage amplifier using a 0.25 μm gate FET.

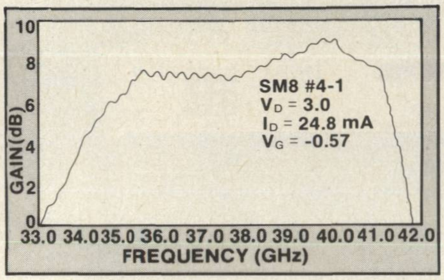

Fig. 5. A 40 GHz amplifier tuned for high frequency.

quency can be rewritten, by using the saturation electron velocity, v_s and gate length L as $f_t \simeq V_s/\pi L$. Since v_s is determined by material, f_T is inversley proportional to the gate length. For example, f_T should improve in theory by roughly a factor of four by reducing the gate length from 1 μm to 0.25 μm.

Recent noise figure and gain results obtained from 0.25-0.3 μm

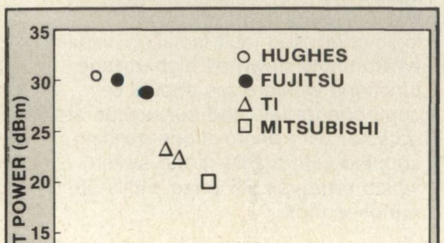

Fig. 6. Reported output power of FETs.

gate length FETs are tabulated in Table I. The data in Table I were obtained as amplifier values and not as device values. The best noise performance from a 0.5 μm gate FET in the 30 GHz range is 3.6 dB with a 4.1 dB associated gain. Comparison of this result with the 0.25 μm gate FET performance indicates a substantial improvement in gain, but not in noise figure. This suggests that further optimization of the 0.25 μm gate FET is needed. By reducing the gate length from 0.5μm to 0.25 μm, substantial gain improvement is clearly illustrated in Figure 1 for the frequency dependent maximum available gain, MAG. The values of MAG were computed from the S-parameters of actual 0.25 μm and a 0.5 μm gate FETs measure over 2-18 GHz. From these S-parameters, a computer optimization determined in equivalent circuit of the FETs from which values of MAG were extrapolated at higher frequencies. Based on the calculated MAG, the current prototype 0.25 μm gate FET should develop 5 dB gain at 60 GHz. Optimization of this FET in terms of both material and device parameters is estimated to result in at least a 2 dB gain improvement.

The 0.25 μm gate is currently defined by a direct write electron beam (E-Beam) microfabrication

[Continued on page 98]

MCL

14 Klystron Amplifiers

Now available with Micro-Processor Control (RS-422 Compatible)

Micro-Processor Controlled Channel Selector Optional

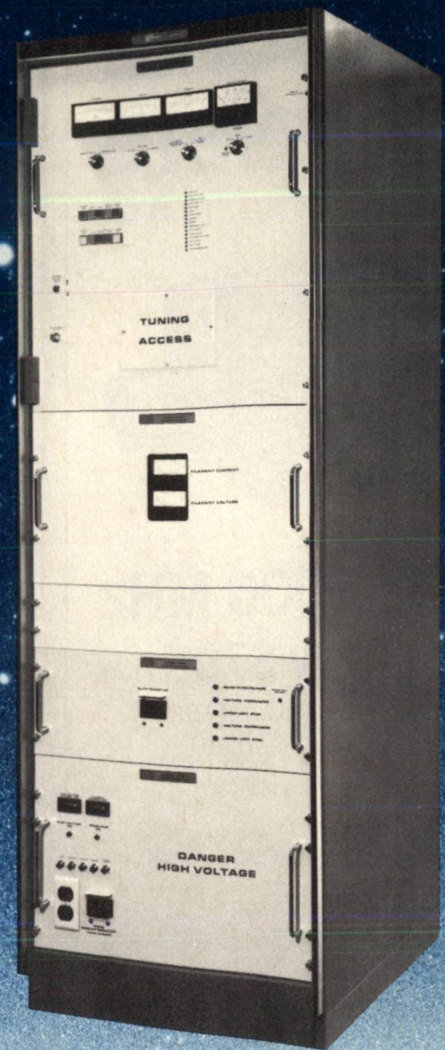

C-Band Frequencies (5.925–6.425 GHz)			
Model Number	Tube Power Out	System Output	System Gain
10538	750 W	+58.4 dBm	75 dB*
10596	750 W	+58.4 dBm	40 dB
10537	1,500 W	+61.4 dBm	75 dB*
10597	1,500 W	+61.4 dBm	40 dB
10587	3,000 W	+64.4 dBm	75 dB*
10598	3,000 W	+64.4 dBm	40 dB
10600	3,350 W	+64.8 dBm	75 dB*
10599	3,350 W	+64.8 dBm	40 dB

*With IPA

KU-Band Frequencies (14.0-14.5GHz)			
Model Number	Tube Power Out (Nominal)	System Output Minimum	System Gain
10578	500 W	+56.4 dBm	70 dB
10605	500 W	+56.4 dBm	33 dB
10586	1,500 W	+60.8 dBm	70 dB
10606	1,500 W	+60.8 dBm	33 dB
10593	2,000 W	+62.0 dBm	70 dB
10607	2,000 W	+62.0 dBm	38 dB

Producing Klystron and TWT amplifiers for commercial satellite earth stations, MCL's engineers have provided solutions to most communication systems' problems. For many years, our engineers have been known as some of the finest microwave problem solvers in the industry.

Two excellent solutions incorporated into our equipment are: CMOS logic-controlled fault isolation circuitry which shuts down all high-voltage functions within 8 ms should key components fail, and our unique arc detector with photo-diode sensing coupled with a PIN-diode switch which removes RF drive within 50 nanoseconds.

Other features include forward/backward fiberoptic inputs which survey the entire waveguide including the Klystron window, plug-in PC boards, color-coded LED status indicators displayed on panel fronts to make trouble-shooting easier and quicker, and beam regulated power supply.

With 8 C-Band units having from 750 W to 3,350 W outputs and system gains up to 75 dB; and 6 KU-Band frequency models with from 500 W to 2,000 W and up to 75 dB system gain, MCL's HPA series amplifiers provide the best answer for your communications systems.

Leading the way in SatCom HPAs

MCL INC

10 North Beach
La Grange, IL 60525
Phone: 312/354-4350
TWX 910-683-1899

CIRCLE 72 ON READER SERVICE CARD

system. The E-beam technology is a very powerful fabrication technique for extremely small gates. The direct E-beam lithography is ultimately capable of defining gate lengths as small as 1500 A. SEM pictures of a 0.25 x 80 μm gate MESFET and magnified view of 0.25 μm gate are shown in Figure 2a and 2b, respectively. This FET was assembled into a hybrid Ka-band amplifier using a prematched network on both input and output circuits. A photograph of the amplifier configuration and the equivalent circuit diagram are shown in Figures 3a and 3b, respectively. The matching network is implemented in close proximity to the FET as seen as in Figure 3a so that an optimum response can be obtained by minimizing circuit losses. The FET is mounted between two short 50 Ω microstrip lines on quartz substrates. As shown in Figure 3a, matching networks which consist of short bond wires terminated by low loss chip capacitors are employed for prematching. The FET is biased through $\lambda/4$ high impedance transmission lines. The measured frequency response of the amplifier is shown in Figure 4 and 5. The results shown in Figure 4 were obtained by tuning for high gain and wide bandwidth. The gain variation of the amplifier is less than 1 dB from 32.2 GHz to 38.2 GHz with a maximum gain of

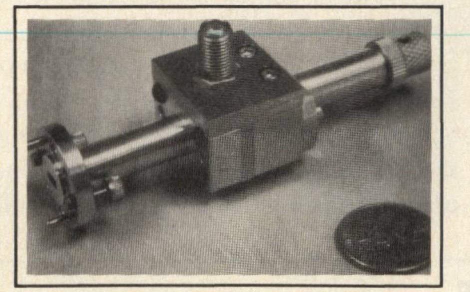

Fig. 7. 70 GHz FET oscillator.

10 dB. When the amplifier was tuned for higher frequency response, the upper frequency was extended to 41 GHz with 7.8 dB gain as shown in Figure 5. The 1 dB bandwidth of the retuned amplifier is 6 GHz. These results imply that the device is capable of high gain even above 41 GHz. Also these performance results clearly establish the FET as a useful millimeter-wave device.

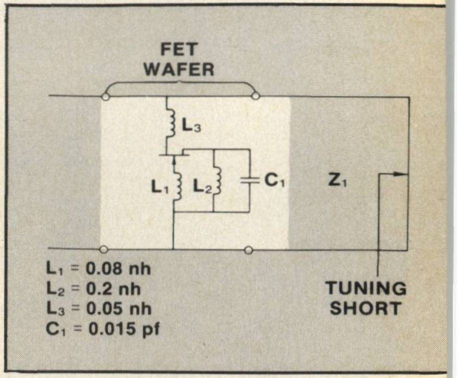

Fig. 8. Equivalent circuit of the FET oscillator.

All of the millimeter-wave performance results described above are for low noise FETs. The situation of the power FET is quite different. The development of millimeter-wave power FETs is much more difficult and progress has been slower. The published output power results from FETs above 18 GHz illustrated in Figure 6. The highest frequency power results, 7mW at 40 GHz and 5 mW at 68 GHz, were measured with an amplifier using a 0.25 μm gate small signal FET and an oscillator using a 0.5 μm gate low noise FET, respectively. The power capabililty of an FET above 30 GHz decreases rapidly with frequency because the required gate width becomes considerably smaller than that used for Ku-band and K-band power FETs. This is primarily due to the device-circuit impedance matching problem. Also as frequency increases, various parasitics associated with FETs, some of which are unimportant at low frequencies, become more serious. In particular a power FET with a large gate width has a serious parasitic problem at these frequencies. The gate width of power FETs for operation above 40 GHz will be less than 200 μm. The output power per unit gate width for millimeter-wave FETs may be similar to the current K-band FETs, which is approximately 0.5 mW/μm, unless an improved device configuration is developed for enhanced power capability. An output power of 100 mW at 44

[*Continued on page 103*]

GHz can be expected from a single FET. In order to further increase the power capability of FETs at millimeter-wave frequencies, an efficient power combiner "approach" must be developed.

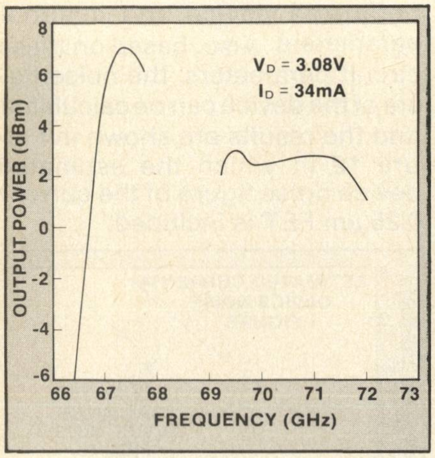

Fig. 9. FET oscillator performance.

The FET oscillator, shown in Figure 7, is constructed using a conventional V-band waveguide circuit originally developed for testing IMPATT diodes. A simplified equivalent circuit of the oscillator is shown in Figure 8. The basic configuration of the oscillator is a modified version of the Colpitts oscillator. The relationship between output power and frequency of oscillation measured from this oscillator is shown in Figure 9 which exhibits two modes of oscillations. In the lower frequency oscillation mode, the output power, depending on the bias voltage, reaches a maximum power of 5 mW with 5% efficiency at 67.5 GHz. In the higher frequency oscillation mode the frequency of oscillation was tunable from 69 to 72 GHz by adjusting the location of the tuning short and was independent of the bias voltage. Considering that the onset of the higher frequency oscillation occurred when the drain bias reached 1.5-2 volts when the generation of high field domains is likely, the Gunn domain phenomenon may play a role in the higher frequency oscillation mode. There was also a strong indication that the lower frequency oscillation may not be a fundamental frequency but rather a second harmonic. In this case, the fundamental frequency of oscillation is under 35 GHz which is below the V-band waveguide cutoff frequency and thus difficult to detect. Regardless of these questions on the mode of oscillation, the demonstrated output power of 5 mW with 5% efficiency at a frequency close to 70 GHz suggests that the operating frequency of FET oscillations may be extended into the 94 GHz range.

Millimeter-Wave Monolithic ICs

Monolithic ICs in the millimeter-wave region are attractive because they can provide the most efficient device curcuit interaction at very high frequencies. The circuit is fabricated directly adjacent to devices so that loss can be minimized. On the other hand, a hybrid approach must deal with interconnection between devices and circuits with either bonding wires or ribbons. They are serious sources of undesirable parasitics at millimeter-wave frequencies. Therefore, at these frequencies the the monolithic integration of devices and circuits offers a considerable advantage in terms of

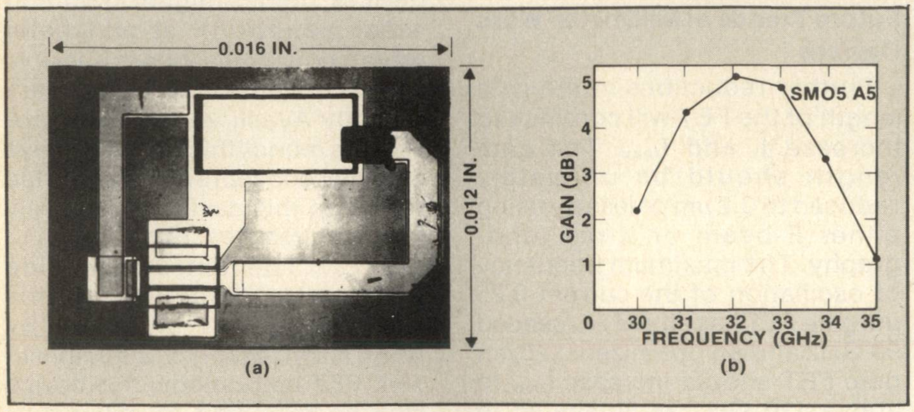

Fig. 10. 32 GHz monolithic amplifier and performance.

[*Continued on page 104*]

[From page 103] **VIABLE APPROACH**

RF performance. This aspect is quite different from the microwave monolithic IC, where the main objective is minimizing cost. The RF performance of a monolithic IC at microwave frequencies does not reach the maximum level achieved by a carefully tuned hybrid circuit. At millimeter-wave frequencies, the required metalization thickness of a monolithic circuit is only about half that of the microwave circuit thus simplifying circuit fabrication and reducing cost. Above all, the size of the millimeter-wave circuit is considerably smaller as compared with the equivalent microwave circuit. For example, the 32 GHz monolithic amplifier shown in Figure 10a has very simple microstrip matching circuits and a DC blocking overlay capacitor. The size of the chip is only 16 x 12 mils. This prototype monolithic amplifier using a 0.5 x 150μm gate FET has demonstrated a maximum gain of 5 dB at 32 GHz as illustrated in Figure 10b. This amplifier can be developed into a very useful low noise RF preamplifier or an IF amplifier by integrating it together with a planar diode mixer in a W-band receiver.

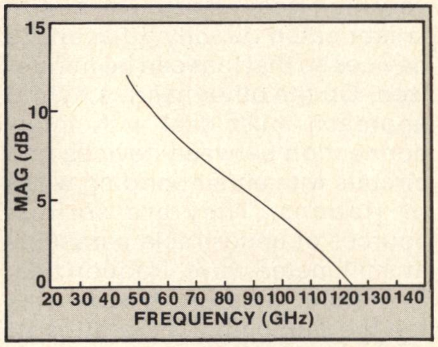

Fig. 11 Computed gain of an optimized ¼ μm gate FET.

Future Trends of Millimeter-Wave Devices

Further reductions in the gate length of the FET will continue to increase f_t and f_{max}. The gate length should be ultimately reduced to 0.2 μm or less by using either E-beam or X-ray lithography. The maximum frequency of oscillation of the current 0.25 μm gate FET has already exceeded 90 GHz and an optimized 0.25 μm gate FET should increase f_{max} to above 120 GHz as illustrated in Figure 11. This projection is obtained by using selectively improved equivalent circuit element values from those used to calculate the frequency dedendent MAG curve shown in Figure 1. The improved circuit element values were estimated from the optimized device and material parameters. Also, based on these circuit parameters, the noise figure of the device can be calculated and the results are shown in Figure 12 in which the estimated device noise figure of the current 0.25 μm FET is included.

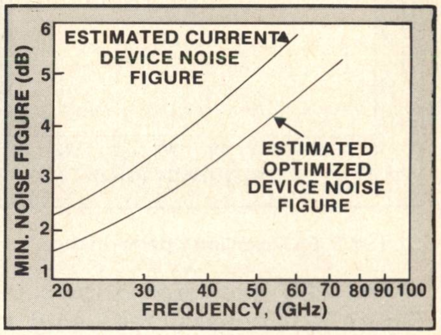

Fig. 12. Minimum noise figure vs. frequency.

It is not expected that a conventional FET with gate lengths of 0.2 μm or less can achieve an f_{max} of 150 GHz. Limitations on high frequency FET performance results from a distributed gate effect. This stems from phase delay of the RF signal as it propagates along the width of the gate. The net effect of the delay is a gain reduction that severely limits high frequency device performance. A possible solution is to design the FET to take advantage of distributed effects. The idea of the distributed device is not new. A FET distributed amplifier was originally proposed by Jutzi[9] 13 years ago. Analyses of such distributed devices predict higher gain and wider bandwidth at millimeter wave frequencies than is possible from conventional FETs. Very recently Ayasli, et. al.[10] has proposed a monolithic traveling wave amplifier concept and has reported works on this device at relatively low frequencies (maximum 13 GHz).[11] The extremely wide bandwidth capability of this approach is very attractive. By using high frequency, subhalfmicron FET technology, this device may be extended to millimeter-wave frequencies.

Several new devices with enhanced high frequency capability have been proposed recently. These include: the permeable base transistor[12] (PBT), the opposed ga source transistor[13] (OGST), vertical short channel FET (V-FET) and the heterojunction FET using GaAlAs/GaAs. The first three devices have unique structures which reduce the effective gate length and minimize the parasitics. These devices are still very new and little experimental data is available to validate their projected high frequency performance required to show their potential RF capability from the actual devices. The estimated f_{max} of those devices is well above 100 GHz and some of the devices are expected to have an f_{max} of up to 300 GHz. The heterojunction FET is an offspring of modulation doping effect.[14] This device known as a high electron mobility transistor (HEMT)[15, 16] because the electron mobility of the active channel layer is extremely high, approximately 10 times higher than that of GaAs at 77° K. This high electron mobility should result in very high f_T. Hence, the HEMT is potentially a very useful millimeter-wave device.

Conclusion

Recent progress in high frequency MESFETs has opened a wide opportunity for these devices to be used in millimeter-wave amplifiers and sources. Low noise and small signal FETs in particular will soon find a rapidly increasing role in the lower millimeter-wave frequency range. Prospects for high power millimeter-wave FETs may not be as bright as the small signal devices. It is necessary to develop an efficient power combining technology to achieve high power capability. The conventional FET will likely be operated as an oscillator at 94 GHz in the near future, but for higher frequency operation other devices must be developed.

Acknowledgement

The author expresses his gratitude to Mr. Ed Watkins for providing the technical data, Mr. Jim Schellenberg for helpful discussions, Dr. T. Midford for reviewing the manuscript.

Some of the results shown in this article were obtained from 0.25 μm gate FETs developed under the contract (Contract No. F33615-79-C-1808) from U.S. Air Force Avionics Laboratory. ■

REFERENCES

1. Shockley, W. "A Unipolar Field Effect Transistor," Proc. IEEE, Vol. 40, P. 1356, (1952)
2. Drangied, K. E., R. Sommerholder, and W. Walter, "High-Speed Gallium-Arsenide Schottky-Barrier Field Effect Transistors," Electron Left., Vol. 6, P. 228 (1970)
3. Krumm, C. F., H. T. Suyematsu, and B. L. Walsh, "A 30 GHz GaAs FET Amplifier", 1978 Technical Paper Digest, IEEE MTT-S International Microwave Symposium, P. 383 (1978)
4. Schellenberg, J. M., G. W. Keithley, C. Kim, V. K. Eu, H. B. Kim, and G. O. Ladd, "RF Characteristics of Ka-Band GaAs FETs" Proc. 1979 Cornell Conf., P. 289 (1979)
5. Schellenberg, J.M., H. Yamasaki, and D. W. Maki, "A 69 GHz FET Oscillator," Technical Paper Digest, 1981 IEEE MTT-S International Microwave Symposium, P. 328 (1981)
6. Watkins, E. T., H. Yamasaki, and J. M. Schellenberg, "40 GHz FET Amplifiers," Tech. Digest 1982 ISSCC, P. 198 (1982)
7. Chu, A., W. E. Courtney, L. J. Mahoney, G. A. Lincoln, R. W. Sudbury, and W.T. Lindley, "GaAs Monolithic Circuit for Millimeter-Wave Receiver Application," Tech. Digest 1981 ISSCC, P. 144 (1981)
8. Yamasaki, H. and G. W. Keithley, "High Performance Low Noise FETs Operating from X-Band through Ka-Band," Tech. Digest 1980 IEDM, P. 106 (1980)
9. Jutzi, W., "A MESFET Distributed Amplifier with 2 GHz Bandwidth," Proc. IEEE (Letters), Vol. 57, P. 1195 (1969)
10. Ayalsi, Y., J. L. Vorhaus, L. Reynolds, and R. A. Pucel, "A Monolithic GaAs Travelling-Wave Amplifier," Electron Left., Vol. 17, P. 413 (1981)
11. Ayasli, Y., J. L. Vorhaus, L. Reynolds, and R.A. Pucel, "A Monolithic GaAs 1 to 13 GHz Traveling-Wave Amplifier," Research, Abst. 1981 GaAs IC Symposium, paper 46, 1981
12. Bozier, C. O. and G. D. Alley, "Fabrication and Numerical Simulation of the permeable Base Transistor," IEEE Trans. On Electron Devices, Vol. ED-27, P. 1128 (1975)
13. Berentz, J.J., G.C. Dalman, and C. A. Lee, "Improved FET Design Reaches Millimeter Waves," Microwaves, Vol. 21, P. 67, 1982
14. Dingle, R., H. L. Stormer, A. C. Gossard and W. Wiegmann, "Electronic Properties of Modulation-Doped GaAs-A1GaAs Heterojunction Super Lattice," 1978 Gallium Arsenide Related Compounds, Inst. Phys. Cof. Ser. No. 45, P. 248, 1979
15. Mimura, T., S. Hiyamiz, H. Hashimoto, and M. Fukuta, "High Electron Mobility Transistors with Selectively Doped GaAs/nA1GaAs Heterojunctions," 1980 Electronic Materials Conf., paper UB-5, (1980)
16. Mimura, T., S. Hiyamiz, K. Toshin and K. Hikosaka, "Enhancement-Mode High Electron Mobility Transistor for Logic Applications," Japan J. Appl. Phys., Vol. 20, P. L317, (1982)

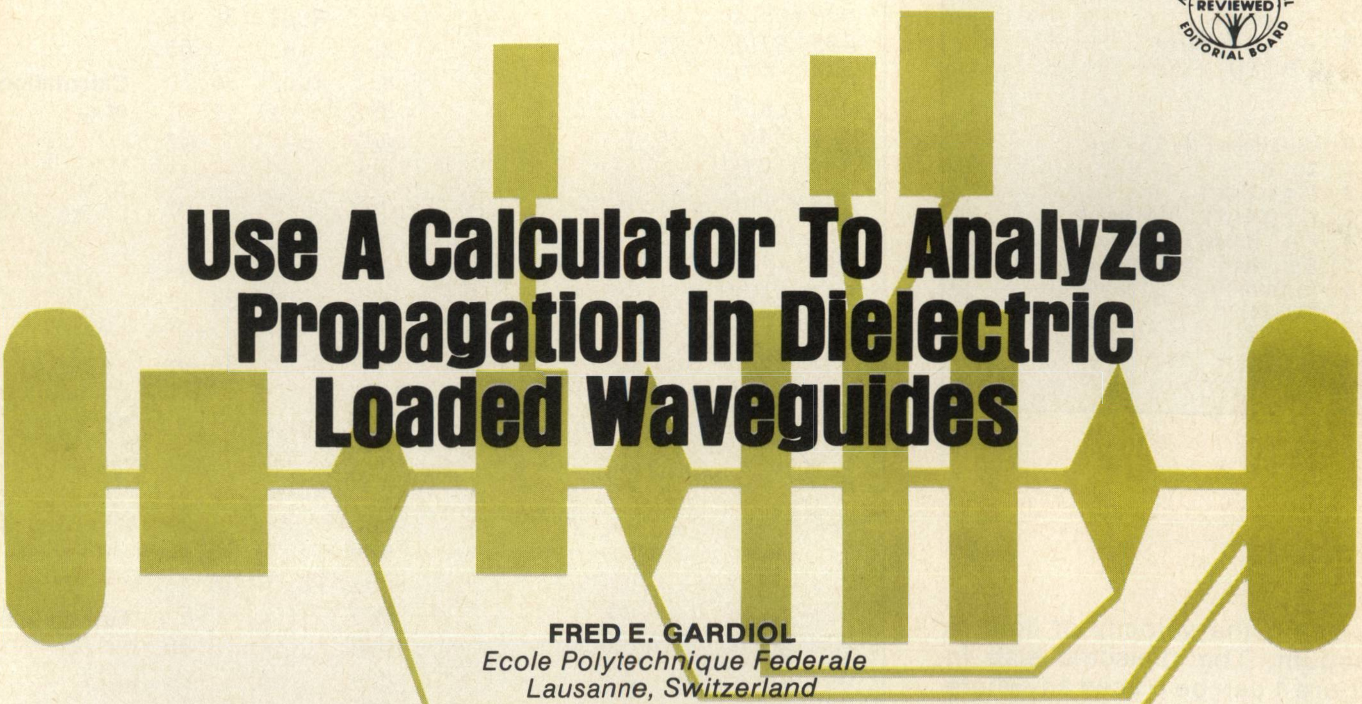

Use A Calculator To Analyze Propagation In Dielectric Loaded Waveguides

FRED E. GARDIOL
Ecole Polytechnique Federale
Lausanne, Switzerland

Rather complex problems have now come within reach of pocket calculators. The program presented here determines the characteristics of a rectangular waveguide loaded with an E-plane dielectric slab on an HP67 or HP97 calculator. The same approach can be used for other problems involving transcendental equations.

INTRODUCTION

Placing a slab of dielectric in a waveguide changes both phase shift and guide impedance. The first effect is utilized to realize phase shifters, the second one to match microwave devices, including isolators, circulators, switches and phase shifters.

The study of wave propagation within the loaded waveguide (Figure 1) has been considered by several authors[1-5]. It leads to a set of transcendental equations, which were first solved graphically (a tedious process), then by pertubation methods (not always accurate) and more recently on a computer. Today, a pocket calculator solves this problem. The program can be stored on a single magnetic program card.

BASIC THEORY

The components of the electromagnetic fields are obtained by solving Maxwell's equations within each homogeneous region, then matched to ensure continuity at the boundaries, yielding the dispersion relation for the dominant mode (distorted TE_{10} mode):

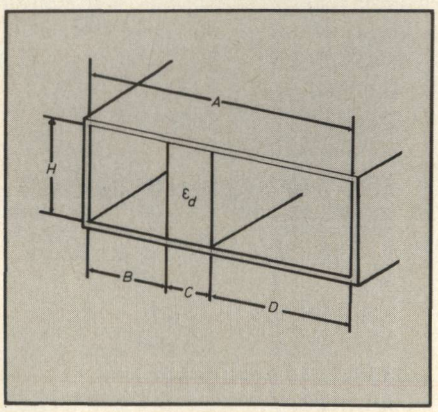

Fig. 1 Rectangular waveguide loaded with one lossless E-plane dielectric slab.

$$h^2 \tan \ell C + h\ell\,(\tan hB + \tan hD) \ldots$$

$$- \ell^2 \tan \ell C \tan hB \tan hD = 0 \qquad (1)$$

where

$$h = \sqrt{k_o^2 - \beta^2} = \frac{2\pi}{c_o}\sqrt{f^2 - f_g^2} \qquad (2)$$

$$\ell = \sqrt{\epsilon_d k_o^2 - \beta^2} \ \ldots$$

$$= \frac{2\pi}{c_o}\sqrt{\epsilon_d f^2 - f_g^2} \qquad (3)$$

$$k_o = \omega\sqrt{\epsilon_o \mu_o} = 2\pi f/c_o \ldots$$

wave number (4)

$\beta = 2\pi/\lambda_g = 2\pi f_g/c_o$ phase shift per unit length (5)

CONTENTS OF THE REGISTERS

A A (mm)
B B (mm)
C C (mm)
D D (mm)
E ε_d (1) relative
I C/A (1)

0 $c_0/2$ then $l\,T_B\,T_D - 1/l$
1 $2\pi/c_0$
2 $f^2\,g$ (GHz^2)
3 f^2 (GHz^2) new value
4 $f'^2 n$ (GHz^2) old value
5 2π then h (mm^{-1})
6 l (mm^{-1})
7 T_B (1)
8 T_D (1)
9 G (1)

$$f_g = c_o/\lambda_g \tag{6}$$

c_0 being the velocity of light in vacuum. The dielectric slab in Figure 1 can be placed anywhere across the waveguide, its relative permittivity ε_d can take any value greater than unity. It is surrounded by two air or vacuum regions. Introducing the three functions:

$$T_B = \frac{\tan hB}{h}, \quad T_D = \frac{\tan hD}{h}, \text{ and}$$

$$T_C = \tan \ell C \tag{7}$$

the relation (1) takes the simplified form:

$$T_C = \frac{T_B + T_D}{\ell T_B T_D - 1/\ell} \tag{8}$$

The calculator solves this equation using an iterative approach. A value of the wavelength λg in the loaded waveguide is specified, and the program determines the corresponding frequency. Starting with an approximate value of the frequency, the right-hand side of (8) is determined. The left-hand side yields a new value for the frequency, which is compared with the starting one. A weighted average of the two is used as starting value for the next step of the

001	*LBLA	21 11	
002	STOA	35 11	
003	RTN	24	
004	*LBLB	21 12	
005	STOB	35 12	
006	RTN	24	
007	*LBLC	21 13	
008	STOC	35 13	
009	RTN	24	
010	*LBLD	21 14	
011	STOE	35 15	**DATA INPUT**
012	RTN	24	
013	*LBLE	21 15	
014	RAD	16-22	
015	DSP3	-63 03	
016	1/X	52	
017	1	01	
018	4	04	
019	9	09	**$c_0/2$ in mm/ns**
020	.	-62	
021	8	08	
022	9	09	
023	6	06	
024	STO0	35 00	
025	2	02	
026	×	-35	
027	×	-35	
028	X²	53	**calculation of f^2_g**
029	STO2	35 02	
030	RCLC	36 13	
031	RCLA	36 11	
032	÷	-24	
033	STOI	35 46	
034	RCLE	36 15	**calculation of G**
035	×	-35	
036	1	01	
037	+	-55	
038	2	02	
039	7	07	
040	X⇄Y	-41	
041	÷	-24	
042	3	03	
043	+	-55	
044	STO9	35 09	**calculation of D**
045	RCLA	36 11	
046	RCLB	36 12	
047	RCLC	36 13	
048	+	-55	
049	−	-45	
050	X<0?	16-45	**test on D**
051	RTN	24	
052	STOD	35 14	
053	Pi	16-24	
054	ENT↑	-21	
055	RCL0	36 00	
056	÷	-24	
057	STO1	35 01	
058	RCLB	36 12	
059	GSB6	23 06	
060	RCLD	36 14	
061	GSB6	23 06	
062	+	-55	
063	RCLI	36 46	
064	+	-55	
065	RCLE	36 15	**Calculation of ε_e**
066	1	01	
067	−	-45	
068	×	-35	
069	1	01	
070	+	-55	
071	√X	54	
072	RCLA	36 11	
073	×	-35	
074	RCL0	36 00	
075	÷	-24	**Calculation of F'_1**
076	1/X	52	
077	X²	53	
078	RCL2	36 02	
079	+	-55	
080	STO3	35 03	
081	RCLI	36 46	
082	.	-62	**Test on C/A**
083	0	00	
084	9	09	
085	X>Y?	16-34	
086	GTO8	22 08	
087	*LBL1	21 01	**Start of loop**
088	RCL9	36 09	
089	.	-62	
090	9	09	
091	7	07	**Reduction of G**
092	Yˣ	31	
093	STO9	35 09	
094	RCL3	36 03	
095	RCLE	36 15	
096	×	-35	**Calculation of ℓ**
097	RCL2	36 02	
098	−	-45	
099	√X	54	
100	RCL1	36 01	
101	×	-35	
102	STO6	35 06	
103	RCL3	36 03	
104	STO4	35 04	
105	RCL2	36 02	
106	−	-45	**Test for hyperbolic dependence**
107	X<0?	16-45	
108	GTO2	22 02	
109	√X	54	
110	RCL1	36 01	
111	×	-35	**Calculation of h**
112	STO5	35 05	
113	RCLD	36 14	
114	GSB7	23 07	
115	STO8	35 08	
116	RCLB	36 12	**Calculation of T_B and T_D**
117	GSB7	23 07	
118	*LBL4	21 04	

```
119 ST07     35 07
120 RCL8     36 08
121  x         -35
122 RCL6     36 06
123  x         -35
124 ST00     35 00
125 RCL6     36 06
126  1/X        52     Calculation
127 ST-0  35-45 00     of Tc
128 RCL7     36 07
129 RCL8     36 08
130  +         -55
131 RCL0     36 00
132  ÷         -24
133 TAN⁻¹    16 43
134 X>0?     16-44     Setting of
135 GTO5     22 05     correct range
136  Pi      16-24     for tan⁻¹ Tc
137  +         -55
138 *LBL5    21 05
139 RCLC     36 13
140  ÷         -24
141 RCL1     36 01
142  ÷         -24
143  X²         53
144 RCL2     36 02     Computation
145  +         -55     of f'n
146 RCLE     36 15
147  ÷         -24
148 RCL4     36 04
149 RCL9     36 09
150  x         -35
151  +         -55     Calculation
152 RCL9     36 09     of f'n+1
153  1          01
154  +         -55
155  ÷         -24
156  √X         54
157 PSE      16 51
158  X²         53
159 ST03     35 03
160 RCL4     36 04     Test on
161 %CH      16 55     frequency
162 ABS      16 31     change
163  .         -62
164  0          00
165  1          01
166 X≤Y?     16-35
167 GTO1     22 01     End of loop
168 *LBL8    21 08
169 RCL3     36 03
170  √X         54
171 PRTX       -14     Print frequency
172 RTN         24
173 *LBL2    21 02
174 CHS        -22     Calculation
175  √X         54     of |h|, TB and TD
176 RCL1     36 01     in hyperbolic case
177  x         -35
```

```
178 ST05     35 05
179 RCLD     36 14
180 GSB3     23 03
181 ST08     35 08
182 RCLB     36 12
183 GSB3     23 03
184 GTO4     22 04
185 *LBL3    21 03
186 RCL5     36 05
187  x         -35     Calculation
188  2          02     of
189  x         -35     tan h (|h|x)
190 CHS        -22        |h|
191  e^x        33
192  1          01
193  +         -55
194  1/X        52
195  2          02
196  x         -35
197  1          01
198  -         -45
199 RCL5     36 05
200  ÷         -24
201 RTN         24
202 *LBL6    21 06
203 RCLA     36 11
204  ÷         -24     Calculation of
205  Pi      16-24     sin (2π X/A)
206  2          02         2π
207  x         -35
208 ST05     35 05
209  x         -35
210 SIN         41
211 RCL5     36 05
212  ÷         -24
213 RTN         24
214 *LBL7    21 07
215 RCL5     36 05
216  x         -35     Calculation of
217 TAN         43     tan (hx)
218 RCL5     36 05        h
219  ÷         -24
220 RTN         24
221 R/S         51
```

[Continued on page 110]

iteration, and process is repeated until the difference between successive frequencies falls below a specified accuracy bound. The frequency is then displayed, and printed on the HP97.

APPROXIMATE VALUE FOR THE FREQUENCY

A good starting point is provided by perturbation theory[1]

$$f_{approx.} = \left\{ f_g^2 + \left(\frac{c_o}{2A}\right)^2 \left[1 + (\epsilon_d - 1) \left[\frac{C}{A} + \frac{\sin(2\pi B/A)}{2\pi} + \frac{\sin(2\pi D/A)}{2\pi}\right]^{-1}\right]\right\}^{1/2} \quad (9)$$

This starting value is a sufficiently accurate approximation (within 1%) for C/A less than 0.09. For larger loadings, the approximation is too rough and the iterative process described in previous section is carried out.

HYPERBOLIC DEPENDENCE OF THE FIELDS IN THE AIR REGIONS

At high frequencies, the term under the square root of (2) becomes negative hence h is a pure imaginary number.[6] The trigonometric functions in (7) become hyperbolic functions. This situa-

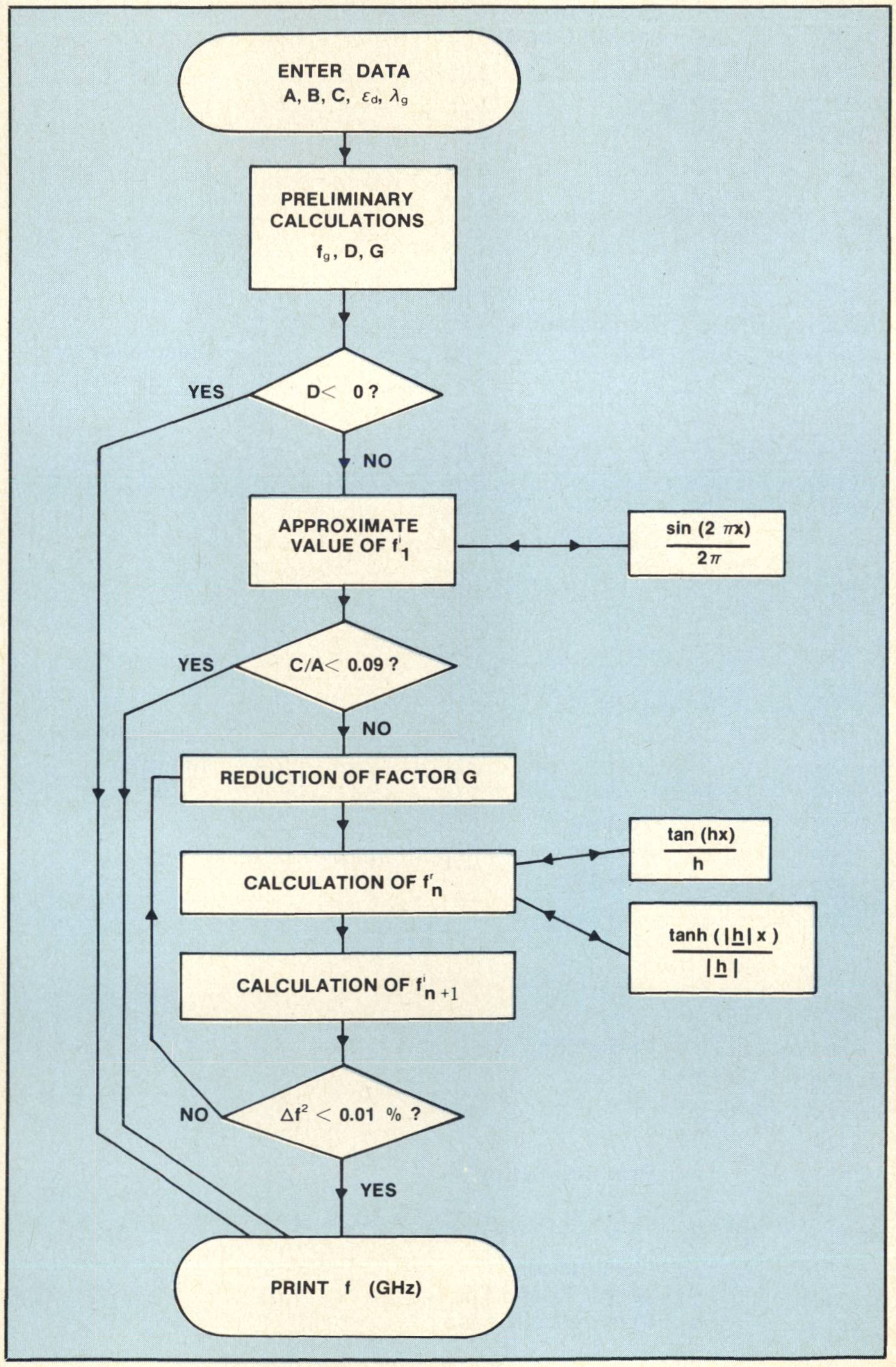

Fig. 2 Flow chart of the calculator program.

tion is detected in the calculator program, the correct dependence is automatically selected.

HOW TO USE THE PROGRAM

- Type the complete listing or introduce a magnetic card on which the program has been recorded (tracks 1 and 2).
- Introduce the waveguide width A in mm and press key A
- Introduce the gap width B in mm and press key B
- Introduce the slab width C in mm and press key C
- Introduce the slab permittivity ε_d and press key D
- Introduce the guide wavelength λ_g and press key E

The calculator then computes the frequency in GHz. At each iteration, the frequency obtained is displayed for one second, allowing one to check the convergence. The computation can be stopped at that point by pressing the R/S key, and resumed by again pressing the R/S key.

The frequency corresponding to another wavelength is obtained by repeating the last step. Any one of the parameters A, B, C and ε_d can be modified independently. The value of λ_g must however be specified before every calculation. A negative result indicates inconsistency in the dimensional data.

CUTOFF OF WAVEGUIDE MODES

For the dominant mode, the cutoff frequency is obtained by specifying a very large wave length. The cut-off frequency of the distorted TE_{20} mode is obtained in a similar manner as for the dominant mode, starting from a frequency about double that of the dominant mode: the calculation is stopped during the first pause (use R/S key), the frequency is doubled and the process re-started (it only works if C/A > 0.09).

As was shown in Reference 7, the first higher-order mode is most often a hybrid mode of the longitudinal section electric (LSE) type. Its cutoff is readily given by this program, simply introducing λ_g = 2H (H = waveguide height). The cut-off frequency of the first longitudinal section magnetic mode (LSM) can be determined with another calculator program (see Reference 8.)

REFERENCES

1. Collin, R. E., *Field Theory of Guided Waves*, New York: McGraw Hill, 1960, p. 228.
2. Hering, K. H., "Quarter Wave Transformer for a Digital Ferrite Phase shifter," *Microwave, Journal.*, Vol. 11, pp. 67-69, January 1968.
3. Gardiol, F. E., "Comments on Quarter Wave Transformer for a Digital Phase-shifter," *Electronics Letters*, Vol. 4, April 1968.
4. Vartanian, P. H., W. P. Ayres, and A. L. Helgesson, "Propagation in Dielectric Slab Loaded Rectangular Waveguide," *IRE Trans. Microwave Theory Tech.*, Vol. MTT-6, April 1958, pp. 215-222.
5. Eberhardt, N., "Propagation in the Off Center E-Plane Dielectrically Loaded Waveguide," *IEEE Trans. Microwave Theory Tech.*, Vol MTT-15, May 1967, pp. 282-289.
6. Bladel, J. Van, and T. J. Higgins, "Cut off Frequency in Two Dielectric Layered Rectangular Waveguides," *Journal. Appl. Phys.*, Vol. 22, March 1951, pp. 329-334.
7. Gardiol, F. E., "Higher-order Modes in Dielectrically Loaded Rectangular Waveguides," *IEEE Trans. Microwave Theory Tech.*, Vol. MTT-16, November 1968, pp. 919-924.
8. Gardiol, F. E., "Careful MIC Design Prevents Waveguide Modes," *Microwaves*, Vol. 16, May 1977, pp. 188-191.

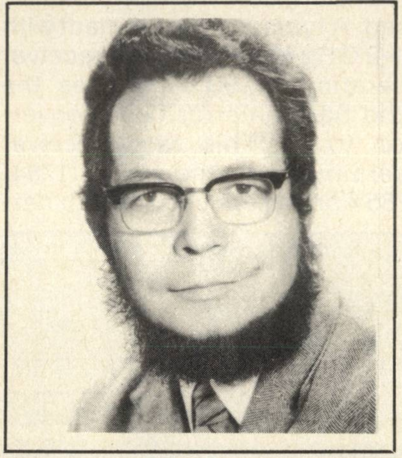

Fred E. Gardiol *was born in Corsier, Switzerland in 1935. He graduated in Physics at Ecole Polytechnique de Lausanne in 1960, received the MSEE degree from the Massachusetts Institute of Technology in 1965 and the Doctorate in Applied Sciences from Louvain University, Belgium in 1969.*

He worked in the semiconductor industry [Transitron, 1960-61] and in microwave ferrite devices [Raytheon SMDO, Waltham MA, 1961-66]. He then joined the staff of Louvain University, Belgium, becoming Assistant Professor in 1969. Since 1970, he is Professor of Electromagnetism and Microwaves at Ecole Polytechnique Federale, Lausanne, Switzerland.

Professor Gardiol is the author of two books in French: Electromagnetisme and Hyperfrequences. He is author or coauthor of more than 100 technical publications. He is a member of IMPI, Sigma Xi, the Swiss Electrotechnical Association [ASE-SEV], the Swiss Association for Space Techniques and the Swiss Alpine Club. He is President of the Swiss Committee of URSI and a Senior Member of IEEE. ■

Cover Story

Millimeter-Wave to Microwave Converter

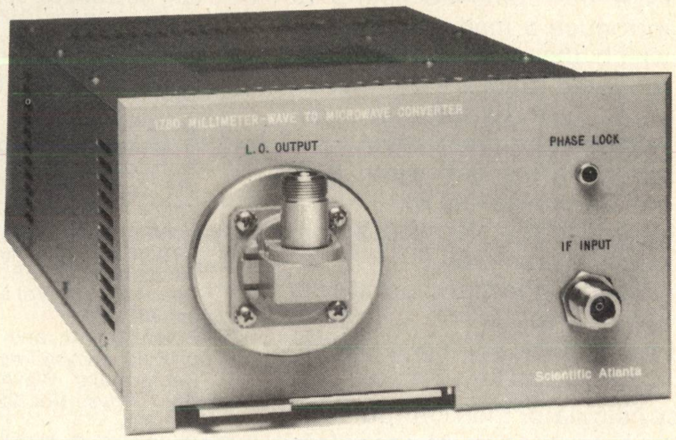

Scientific Atlanta
Atlanta, GA

Features

- Downconverts Millimeter-wave signals in the 33 GHz to 107.05 GHz band to signals in the 1 to 4 GHz band for input to broadband measurement receivers.
- Operation over all popular frequency ranges from 33 GHz to 107.05 GHz.
- Up to three coherent channels of operation for phase and amplitude measurements.
- Improves Millimeter-wave sensitivity and operating dynamic range of measurement receivers up to 30 dB.
- Converters and mixers can be remoted to reduce RF cable losses.

Description

The Model 1784/1785 Millimeter-to-Microwave Converters permit standard single-channel and multi-channel microwave measurement receivers to perform with excellent sensitivity at millimeter-wave frequencies in the 33.0 GHz to 107.05 GHz band. The converters can be used with any Scientific-Atlanta or equivalent microwave receiver operating over the 1.0 GHz to 4.0 GHz frequency range.

Millimeter-to-microwave converters overcome conversion losses associated with microwave measurement receivers operating at high mixer harmonic numbers. By using an X-band (11.45 GHz) local oscillator in the converter, lower harmonic numbers can be used. A typical measurement with a 1-2 GHz local oscillator receiver operating at 90 GHz uses the 42nd harmonic for downconversion to IF. This same receiver operating with the Model 1784/1785 converters uses the 8th harmonic for 90 GHz. Operating at this lower harmonic reduces conversion loss and noise associated with the mixing process and increases measurement sensitivity.

The Model 1784 basic converter consists of an X-band fundamental local oscillator (frequency = 11.450 GHz.) This local oscillator is phase locked to a 949.22

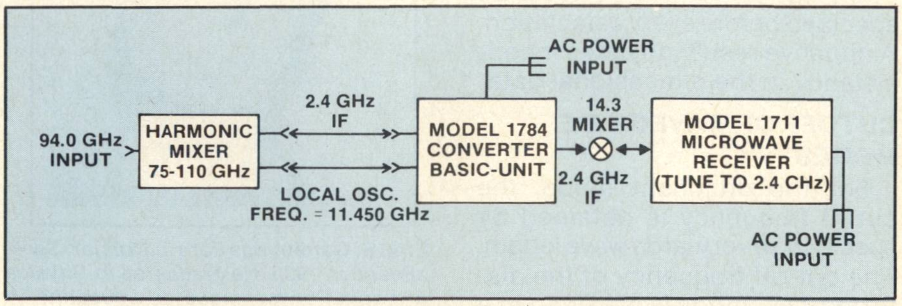

Fig. 1 Block diagram of single-channel receiving system.

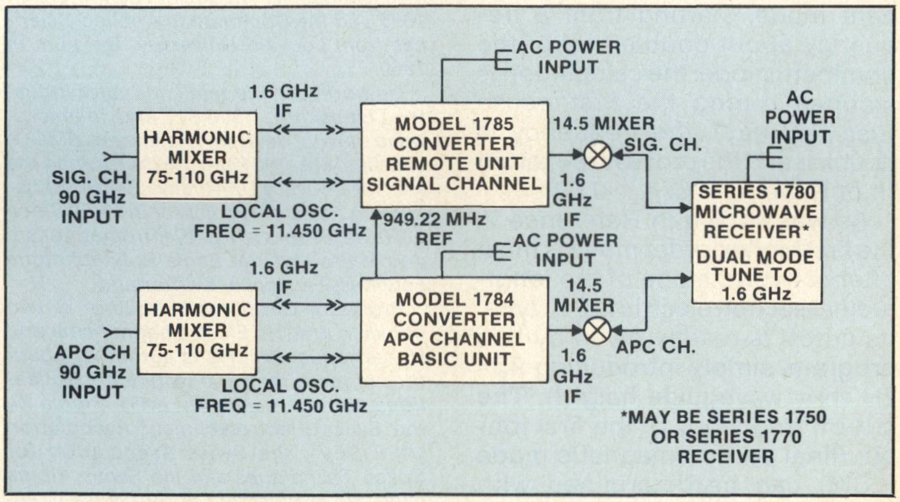

Fig. 2 Block diagram of coherent two-channel receiving system.